RESEARCH PAPER

Acta Neurobiol Exp 2026, 86
DOI: 10.55782/XXX

# Projections from thalamic nucleus reuniens to medial septum enable extinction of remote fear memory

**Kamil F. Tomaszewski, Olga Gajewska-Woźniak, Magdalena Ziółkowska, Kacper Łukasiewicz, Anna Cały, Narges Sotoudeh, Monika Puchalska, Ahmad Salamian and Kasia Radwanska***

*Laboratory of Molecular Basis of Behavior, Nencki Institute of Experimental Biology of Polish Academy of Sciences, Warsaw, Poland*
** Email: k.radwanska@nencki.edu.pl*

Aversive experiences lead to the formation of long-lasting memories. Despite the need to better understand how enduring fear memories can be attenuated, the underlying brain circuits remain largely unknown. In this study, employing a combination of genetic manipulations, neuronal circuit mapping, and chemogenetics in mice, we identify a new projection from the thalamic nucleus reuniens (RE) to the medial septum (MS), and show that this circuit is involved in the extinction of remote (30-day old), but not recent (1-day old), fear memories. We also demonstrate that the activity of this circuit, as well as consolidation of remote extinction memory, require autophosphorylation of αCaMKII, a key signaling molecule in the excitatory synapses. Our findings provide the first functional description of the RE→MS circuit and highlight the significance of the thalamo-septal regions in memory organization as a function of memory age, a phenomenon known as systems consolidation.

**Key words:** nucleus reuniens, medial septum, fear extinction, remote memory, systems consolidation, thalamo-septal circuit, αCaMKII autophosphorylation

## INTRODUCTION

The distinction between dangerous and safe contexts, as well as the ability to update such information in a changing environment is crucial for animal survival, as mistakes can have costly consequences. Impairments in context-dependent behaviors have been associated with pathological conditions including post-traumatic stress disorder, schizophrenia, and substance abuse disorders (Maren et al., 2013; Garfinkel et al., 2014; Lissek et al., 2014; Grodin et al., 2018). Therefore, understanding the molecular and cellular mechanisms that underlie the updating of contextual memories is vital for developing new therapeutic approaches (Myers & Davis, 2002; Maren & Quirk, 2004; Ji & Maren, 2007).

Contextual fear conditioning (CFC) represents a method to study contextual memories in laboratory animals (Maren et al., 2013). In this approach, a spatial context, the conditioned stimulus (CS), is repetitively paired with an aversive unconditioned stimulus (US), such as a mild electric shock. The observable freezing behavior serves as a measurable indicator of contextual fear memory. As exposure to the CS persists without the US, freezing behavior typically diminishes, accompanied by increased exploratory behavior. This process, known as fear extinction, unfolds as animals gradually recognize that the context no longer predicts impending shocks. To facilitate extinction, mice must actively retrieve and revise contextual memories, necessitating the presence of specific brain mechanisms. The "classic" neuronal circuit of contextual fear extinction includes medial prefrontal cortex (mPFC), amygdala, and hippocampus (Orsini & Maren, 2012; Maren et al., 2013). However, the brain regions that contribute to memory recall may vary with memory age. In particular, memories for events initially depend upon the hippocampus, with time these memories become increasingly

*Received 14 January 2026, accepted 4 February 2026*

dependent upon the cortex for their expression (Buzsáki, 1996; Kitamura et al., 2017; Tonegawa et al., 2018). Post-learning communication between the hippocampus and cortex, *via* the thalamus, is thought to drive this time-dependent reorganization process called systems consolidation (Simons & Spiers, 2003; Frankland & Bontempi, 2005; Moscovitch et al., 2006; Ji & Maren, 2007; Preston & Eichenbaum, 2013; Wheeler et al., 2013; Tanaka et al., 2014; Vetere et al., 2021). This indicates that the extinction of remote memories may similarly rely on a re-distributed network, likely requiring additional players to the canonical extinction-mediating pathways of recent memories.

Here, we used c-Fos immunostaining to study neuronal correlates of recent (1 day) and remote (30 days) memory extinction. The analysis revealed a number of regions hyperactivated during extinction of remote memory, including cortical, thalamic, hippocampal and amygdalar areas. While the contributions of hippocampal and cortical regions to fear extinction have been studied in detail, much less is known about how thalamic regions contribute to this memory reorganization process at different post-encoding delays. Accordingly, we focus here on the thalamic nucleus reuniens (RE) and medial septum (MS). We identified projections from RE to MS (RE→MS) and showed that RE, MS and the RE→MS pathway are necessary for extinction of the remote, but not recent, contextual fear memory. Previous studies identified RE projections to the CA1 area that are involved in extinction of recent contextual fear memory (Ratigan et al., 2023; Totty et al., 2023; Ziółkowska et al., 2025) and RE projections to the basolateral nucleus of the amygdala (BLA) to be involved in extinction of remote fear memories (Silva et al., 2021). Current results indicate a novel thalamo-septal pathway that is specifically engaged in the updating of remote memories. Our discoveries suggest that, akin to memory consolidation, the brain circuits involved in fear extinction undergo a spatial reorganization over time.

Calcium and calmodulin-dependent kinase II (CaMKII) is one of the key synaptic molecules that contributes not only to formation and updating of recent contextual memories but also to systems consolidation of remote memories (Giese et al., 1998; Frankland et al., 2001; Kimura et al., 2008; Radwanska et al., 2011, 2015; Wheeler et al., 2013). In particular, knock-in mice with a targeted Threonine 286 mutation to Alanine (T286A), that prevents the autophosphorylation of αCaMKII, have impaired formation and extinction of contextual memories (Giese et al., 1998; Irvine et al., 2005, 2006; Kimura et al., 2008; Radwanska et al., 2011, 2015), while heterozygous αCaMKII knock-out mice (αCaMKII$^{+/-}$) have spared recent memory but severely impaired its long-term (>10 days) retention (Frankland et al., 2001). Here, we tested the effect of heterozygous T286A mutation (T286A$^{+/-}$) on extinction of recent and remote contextual fear memory. As T286A$^{+/-}$ mutant mice showed impaired extinction of remote, but not recent, contextual fear memory, we used c-Fos immunostaining in this mouse model to study neuronal correlates of remote memory impairment. The analysis revealed that both MS and RE were hyperactivated and their activity was decorelated in the heterozygotes specifically during extinction of remote memory. Hence, our data additionally indicate that the autophosphorylation of αCaMKII regulates neuronal network reorganisation that is necessary for consolidation of remote extinction memory.

# METHODS

## Animals

T286A$^{+/-}$ and WT mice were obtained from crossing heterozygous αCaMKII autophosphorylation-deficient mutant mice (αCaMKII-T286A$^{+/-}$) (Giese et al., 1998) and heterozygotes of Thy1-GFP(M) line (Thy1-GFP$^{+/-}$) (Feng et al., 2000) at the Nencki Institute animal house, and genotyped as previously described (Giese et al., 1998; Feng et al., 2000). Homozygous Ai14 mice were genotyped as previously described (Madisen et al., 2010) and crossed with C57BL/6J animals. Heterozygotes were used in the experiment. C57BL/6J male mice were purchased from the Medical University of Białystok, Poland. Mice were 10 weeks-old at the beginning of the training. The animals were maintained on a 12 h light/dark cycle with food and water *ad libitum*. Mice were housed in standard home cages (dimensions: 267 × 207 × 140 mm), 4-6 mice per cage. After stereotactic surgeries mice were housed individually (cage dimensions: 369 × 156 × 132 mm) for 3 days and afterwards they were moved back to group cages. Behavioral experiments were conducted in the light phase of the cycle. Naive/control animals (same age and lines as experimental mice) were group housed 4-6 animals per cage. All procedures conducted in the study were approved by the 1st Local Ethical Committee, Warsaw, Poland (permission number: 261/2012 and 529/2018).

## Contextual fear conditioning (CFC)

Mice were trained in a conditioning chamber located in a soundproof box (Med Associates Inc., St. Albans, VT, USA). The chamber floor had a stainless steel grid for shock delivery. Before and after each training ses-

sion, chambers were cleaned with 70% ethanol, and paper towels soaked in ethanol were placed under the grid floor. A video camera was fixed inside the door of the sound attenuating box, for the behavior to be recorded. Freezing behavior (defined as complete lack of movement, except respiration) and locomotor activity of mice were automatically scored with VideoFreeze Software (Med Associates Inc.). The experimenters were blind to the experimental groups.

On the day of CFC, mice were brought to the conditioning room 30 minutes before the training. Animals were placed in the chamber, and after a 148-second introductory period, a foot shock (2 seconds, 0.70 mA) (US) was presented. The shock was repeated five times, with intertrial interval of 90 seconds. Thirty seconds after the last shock, mice were returned to the home cage. Mice of the 5US groups were sacrificed 24 hours after the initial training. For the extinction of contextual fear, mice were re-exposing to the conditioning chamber without US presentation for 20 (WT and T286A$^{+/-}$ animals) or 30 minutes (C57BL/6J mice) either 1 or 30 days after the training (extinction of recent and remote memory, respectively). WT and T286A$^{+/-}$ mice from the Extinction groups were sacrificed 70 minutes after the extinction session. To test the efficiency of extinction, mice were re-exposed to the training context 24 hours after the extinction session for an additional 5 minutes. The differences in the length of the extinction session used for T286A$^{+/-}$ animals and C57BL/6J mice resulted from the fact that while for the WT/T286A$^{+/-}$ mice a 20 minute-long extinction session efficiently decreased freezing during the test, we did not see such effect for the C57BL/6J mice. Accordingly, we had to adjust the extinction protocol for these mice.

*CNO administration*

For intraperitoneal (i.p.) injections, Clozapine N-Oxide (CNO) was dissolved in 0.9% saline. If not stated otherwise, CNO (3 mg/kg) was injected 30 minutes prior to the contextual fear memory extinction session.

## c-Fos immunoreactivity

The mice were anesthetized with a mixture of Ketamine/Xylazine (90 mg/kg and 7.5 mg/kg respectively, (i.p.) Biowet Puławy) and next sedated with sodium pentobarbital (50 mg/kg intraperitoneal (i.p.) and perfused transcardially with 20 ml of PBS (Phosphate-buffered saline; POCH, Poland), followed by 50 ml of 4% paraformaldehyde (PFA; Sigma-Aldrich, Poland) in 0.1 M PBS, pH 7.5. Brains were stored in the same solution for 24 h at 4°C. Next, the brains were transferred to the solution of 30% sucrose in 0.1 M PBS (pH 7.5) and stored at 4°C for 72 h. Brains were frozen at -20°C and coronal sections (40 µm) cut in the frontal plane on a cryostat microtome (YD-1900, Leica). Coronal slices were stored in -20°C in PBSAF (PBS, 15% sucrose, 30% ethylene glycol, 0.05% $NaN_3$). Every sixth section through the whole brain was used for immunostaining. Sections were washed three times for 6 min in PBS, followed by incubation in blocking solution (5% NDS, Merck S30-M; 0.3% Triton X-100; Sigma Aldrich) in PBS for 2 h at room temperature (RT). Next, sections were incubated with c-Fos polyclonal antibody (sc-52; Santa Cruz Biotechnology, 1: 1000) for 12 h in 37°C, washed three times in PBST (0.3% Triton X-100 in PBS) and incubated with secondary antibody (1: 500) conjugated with Alexa Fluor-594 (Invitrogen A-11062) for 2 h at room temperature. After incubation with the secondary antibody sections were washed three times for 6 min in PBS and mounted on microscopic slides covered with mounting dye with DAPI (Invitrogen, 00-4959-52).

## c-Fos quantification

c-Fos immunostaining was imaged under a confocal microscope (Leica TCS SP5; objective 10×) and fluorescent microscope (Olympus VS120; objective 10×). Cells were considered positive for c-Fos immunoreactivity if the nucleus had an area ranging from 5 to 160 µm$^2$, and was significantly distinct from the background. c-Fos$^+$ cells were counted in 23 brain regions. We took 2 to 8 microphotographs for each animal per each brain region, resulting in 9 to 48 pictures per experimental group per brain region. Microphotographs were converted into an 8-bit grayscale and the same threshold used for a selected area of interest. The densities of the nuclei were counted with the ImageJ software (National Institute of Health, Bethesda, MD) by an experimenter blind to the experimental condition. The position of the analyzed brain regions was determined according to the mouse brain atlas (Paxinos and Franklin, 2019) (Supplementary Fig. 1B-C).

## Stereotactic surgery

Mice were anesthetized with isoflurane (5% for induction, 1.5-2.0% after) and fixed in the stereotactic frame (51503, Stoelting, Wood Dale, IL, USA). $AAV_{2.1}$ [camk2a_mCherry (titer 7.5 × 10$^7$ pc/µl, from Karl Deisseroth's Lab, Addgene plasmid #114469); hSyn_hM4D(Gi)_mCherry (4.59 × 10$^9$ pc/ul; Addgene plasmid #50475)] were injected into RE (250 nl, coordinates from the Bregma: AP, -0.58 mm; ML, ±0.1 mm; DV,

-4.3 mm), MS (150 nl, coordinates from the Bregma: AP, -0.75 mm; ML, ± 0.0 mm; DV, -4.1 mm), $AAV_9$: hSyn_DiO_hM4Di-mCherry ($3.3 \times 10^9$ pc/µl; constructed by the VVF [dlox-hM4D(Gi)_mCherry(rev)-dlox: Addgene #50461]) and $AAV_9$: hSyn_DIO_mCherry ($3.4 \times 10^9$ pc/µl; constructed by the VVF) and $AAV_9$: camk2a_hM4D(Gi)_mCherry ($4.4 \times 10^9$ pc/ul; Addgene plasmid #50477) were injected into RE; $rAAV_1$: iCre_EGFP ($3.6 \times 10^9$ pc/µl) constructed by the VVF [iCre: Addgene #24593] and $rAAV_1$: hSyn-EGFP ($1.7 \times 10^{11}$ pc/µl) was injected into the MS (Paxinos and Franklin, 2019). We used beveled 26 gauge metal needle and 10 µl microsyringe (SGE010RNS, WPI, USA) connected to a microsyringe pump (UMP3, WPI, Sarasota, USA), and its controller (Micro4, WPI, Sarasota, USA) with an injection rate 0.1 µl/min. After injection, the needle was left in place for an additional 10 min to prevent unwanted spread of the vector. The AAVs were prepared by the Laboratory of Animal Models at Nencki Institute of Experimental Biology, Polish Academy of Sciences and Viral Vector Facility of ETH Zurich. Efficient and specific viral expression was assessed on the brain sections after all experiments. Only mice with AAVs in the regions of interest were used in the statistical analyses.

### Statistics

Analysis was performed using Graphpad Prism 9.5.1. All the statistical details of experiments can be found in the legends of the figures. Data with normal distribution are presented as mean ± standard error of the mean (SEM) or as median ± interquartile range (IQR) for the population with non-normal distribution. When the data met the assumptions of parametric statistical tests, results were analyzed by one- or repeated measures two-way ANOVA (RM ANOVA), followed by Tukey's or Fisher's *post hoc* tests, where applicable. Differences in means were considered statistically significant at $p<0.05$.

## RESULTS

### Neuronal correlates of recent and remote fear extinction

To test extinction of recent and remote fear memories, mice underwent contextual fear conditioning (CFC) in a novel context, consisting of five electric foot shocks (unconditioned stimuli, US). Freezing levels were low at the beginning of CFC but progressively increased over the course of training. One or thirty days after conditioning, animals were re-exposed to the training context to induce extinction of recent or remote fear memories, respectively. At the beginning of the extinction sessions, freezing levels were high in both the Recent and Remote groups, confirming successful formation of contextual fear memory, and subsequently decreased within the session. Fear extinction memory was tested one day after the extinction session. In both groups, mice exhibited a significant reduction in freezing during the test session (T) compared to the beginning of extinction (E5), indicating successful formation of extinction memory. Notably, mice that underwent remote extinction showed a greater reduction in freezing than those in the recent group (Fig. 1A–C).

To identify neural correlates of recent and remote fear extinction, a separate cohort of mice underwent CFC followed by an extinction session either 1 or 30 days later (Recent and Remote groups, respectively). Animals were sacrificed 70 minutes after the extinction session (Supplementary Fig. 1A). Brain sections were prepared for immunofluorescent detection of c-Fos protein as a marker of neuronal activity. c-Fos expression was quantified across 23 brain regions spanning

Fig. 1. Neuronal correlates of recent and remote fear extinction. (A) Experimental timeline and summary of data for freezing levels during the extinction of recent and remote contextual fear memory (n=6 per group). Mice underwent CFC (CFC: RM ANOVA, effect of time: $F_{(1,10)}=236$, $P<0.001$; effect of extinction delay: $F_{(1,10)}=0.293$, $P=0.600$; time × extinction delay: $F_{(1,10)}=2.20$, $P=0.169$), followed by recent or remote fear memory extinction session (Extinction: RM ANOVA, effect of time: $F_{(1.24,\ 11.2)}=7.30$, $P=0.016$; effect of extinction delay: $F_{(1,9)}=1.25$, $P=0.292$; time × extinction delay: $F_{(3,27)}=0.078$, $P=0.971$) and fear extinction test on the next day (Test: unpaired t-test: $t(10)=0.578$, $P=0.576$). (B-C) Summary of data showing freezing levels during the first 5 minutes of the extinction session (E5) and test (T) (RM ANOVA, effect of time: $F_{(1,10)}=25.33$, $P<0.001$; effect of extinction delay: $F_{(1,10)}=0.519$, $P=0.49$; time × extinction delay: $F_{(1,10)}=1.728$, $P=0.22$), and the change of freezing frequency during T as compared to E5 (unpaired t-test: $t(10)=1.314$, $P=0.22$). (D). Fold change of the c-Fos signal density, where the recent (Rec) and remote (Rem) extinction groups are compared to mice sacrificed 24 hours after CFC (5US) or to each other (n=6 per group, 8-37 sections per region per group). (E) Significant change of the c-Fos signal density (based on FDR results). (F, G) Correlation matrix of c-Fos density signal for mice sacrificed after Recent and Remote extinction (based on P values for Spearman correlations). PrL, prelimbic cortex; IL, infralimbic cortex; CG, cingulate cortex; RSG, retrosplenial cortex, granular part; RSA, retrosplenial cortex, agranular part; V1, primary visual cortex; ENT, entorhinal cortex; LS, lateral septum; MS, medial septum; AD, anterodorsal nucleus of thalamus; AV, anteroventral nucleus of thalamus; AM, anteromedial nucleus of thalamus; LD, laterodorsal nucleus of thalamus; RE, nucleus reuniens; CM, centromedial nucleus of thalamus; MD, mediodorsal nucleus of thalamus; PV, paraventricular nucleus of thalamus; CA1, dorsal hippocampus, CA1 area; CA3, dorsal hippocampus, CA3 area; DG, dentate gyrus; BLA, basolateral nucleus of the amygdala; LA, lateral nucleus of the amygdala; CeA, central nucleus of the amygdala, capsular and lateral divisions; CeM, central nucleus of the amygdala, centromedial division.

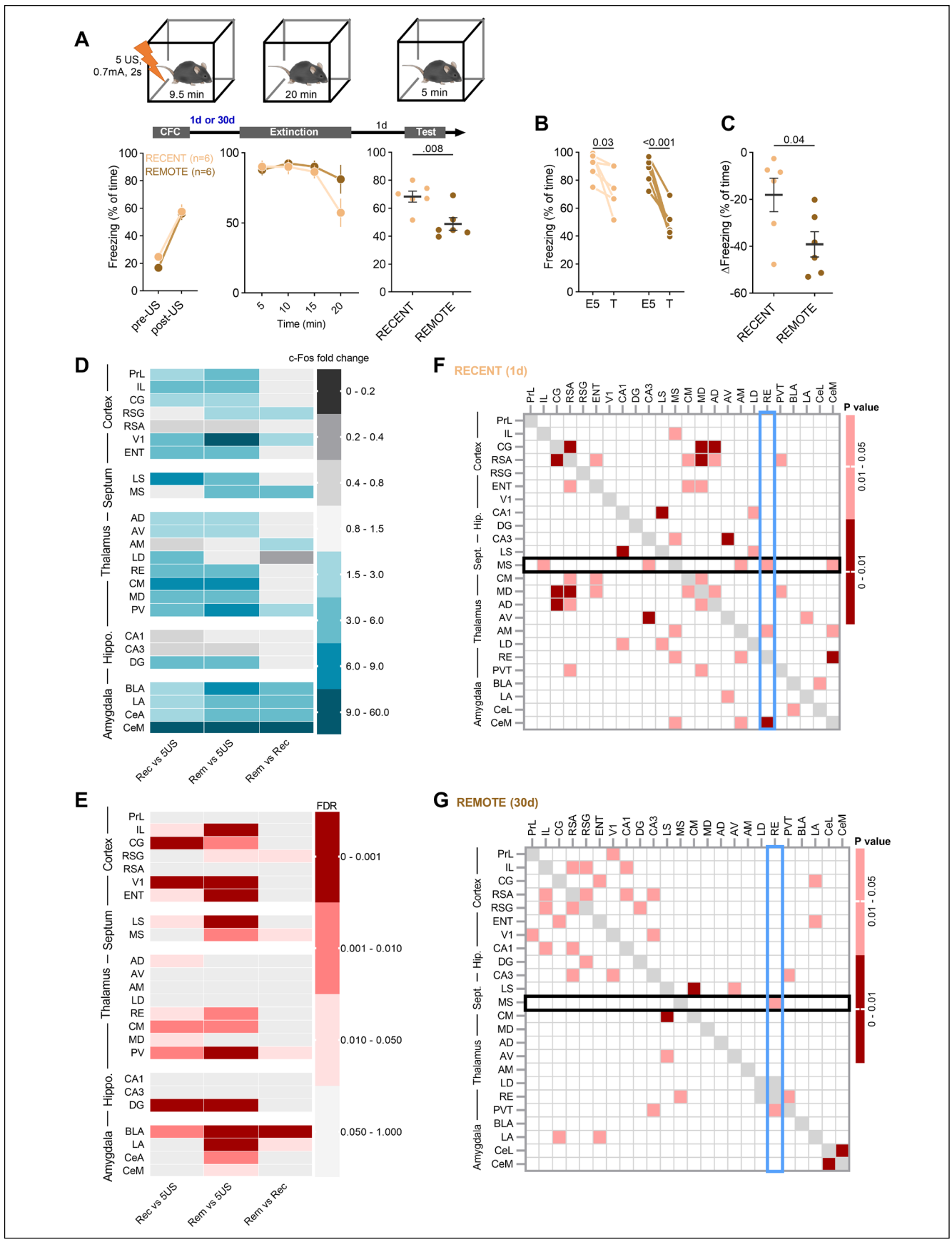
A
5 US,
0.7mA, 2s
9.5 min
20 min
5 min
1d or 30d
CFC
Extinction
1d
Test
RECENT (n=6)
REMOTE (n=6)
Freezing (% of time)
pre-US
post-US
Time (min)
.008
RECENT
REMOTE
B
0.03
<0.001
E5 T
E5 T
C
0.04
ΔFreezing (% of time)
RECENT
REMOTE
D
c-Fos fold change
Cortex
Septum
Thalamus
Hippo.
Amygdala
PrL
IL
CG
RSG
RSA
V1
ENT
LS
MS
AD
AV
AM
LD
RE
CM
MD
PV
CA1
CA3
DG
BLA
LA
CeA
CeM
0 - 0.2
0.2 - 0.4
0.4 - 0.8
0.8 - 1.5
1.5 - 3.0
3.0 - 6.0
6.0 - 9.0
9.0 - 60.0
Rec vs 5US
Rem vs 5US
Rem vs Rec
E
FDR
0 - 0.001
0.001 - 0.010
0.010 - 0.050
0.050 - 1.000
F
RECENT (1d)
Sept.
Hip.
P value
0.01 - 0.05
0 - 0.01
G
REMOTE (30d)

the dorsal hippocampus, amygdala, cortex, thalamus, and septum (Supplementary Fig. 1B).

Overall, both recent and remote extinction were associated with a significant increase in c-Fos expression across multiple brain regions compared to the 5US control group (Fig. 1D–E). These changes were more robust following remote extinction: significant elevations in c-Fos were observed in 12 regions after recent extinction and in 15 regions after remote extinction. In five regions—RSG, MS, PV, BLA, and LA—c-Fos levels were significantly higher in the Remote than in the Recent group. While the contributions of amygdalar and cortical regions in contextual fear extinction have been studied in detail, much less is known about how thalamic regions contribute to this memory reorganization process at different post-encoding delays. We therefore decided to focus, in the following experiments, on the role of MS in recent and remote memory extinction.

Additionally, we found that the patterns of inter-regional c-Fos levels correlations differed between the Recent and Remote groups (Fig. 1F–G). Remote extinction was characterized by co-activation of cortical and hippocampal regions, whereas recent extinction primarily engaged septal, thalamic, and cortical regions. Interestingly, at both timepoints, MS activity correlated with RE, suggesting functional interactions between these structures.

## Validation of the chemogenetic tools

To validate MS function in fear extinction we used a chemogenetic approach relying on the combination of Gi-protein-coupled inhibitory DREADDs (Designer Receptors Exclusively Activated by Designer Drugs) (hM4Di) and hM4Di agonist, clozapine N-oxide (CNO) (Gomez et al., 2017; Jendryka et al., 2019). As a recent study showed that CNO is reverse-metabolized to clozapine and produces clozapine-like effects (Manvich et al., 2018), we first tested the effect of CNO on remote fear memory extinction. C57BL/6J mice (without hM4Di expression) underwent CFC and 30 days later they were injected with CNO (0.5, 3 or 10 mg/kg) or saline. Thirty minutes later they were exposed to the training context for contextual fear memory extinction and fear extinction memory was tested in the same context one day later. We observed no effect of CNO on fear memory recall during the Extinction session, or fear extinction memory during the test (Supplementary Fig. 2A-C).

To test the efficiency of the chemogenetic manipulation to inhibit fear extinction-induced c-Fos expression, a new cohort of mice was injected into V1 with adeno-associated viral vectors (AAVs) encoding hM4Di and red fluorescent protein, mCherry, under human synapsin (*hSyn*) promoter allowing for neuron-specific transgene expression (Kügler et al., 2003). As a control AAV encoding only mCherry was used. Three weeks post-surgery and viral transduction, mice underwent CFC, followed 30 days later by a contextual fear extinction session. Mice were injected with CNO (i.p., 3 mg/ kg) 30 minutes prior to the Extinction and they were sacrificed 60 minutes after the Extinction session. Their brains were sliced and immunostained to detect c-Fos protein. The statistical analysis of the data revealed significantly lower frequency of c-Fos-positive (c-Fos$^+$) nuclei among the cells transduced with hM4Di as compared to the mCherry controls indicating that chemogenetic manipulation effectively prevented c-Fos expression, hence blocked cell activity (Supplementary Fig. 2D-E).

## Contribution of MS to extinction of contextual fear memory

While, former studies showed that MS contributes to recent fear memory formation and extinction (Calandreau et al., 2007; Tronson et al., 2009; Jiang et al., 2016; Knox, 2016; Knox & Keller, 2016; Knox et al., 2016), our analysis indicates that MS activity during extinction increases as the memory age. To test the role of the MS in remote fear memory extinction, C57BL/6J mice were injected into the MS with AAVs encoding hM4Di or mCherry (Fig. 2A–B). Three weeks after surgery and viral transduction, mice underwent CFC, followed by a Recent or Remote extinction session conducted 1 or 30 days after CFC, respectively. Prior to extinction, mice received an intraperitoneal injection of CNO (3 mg/kg).

Freezing levels increased during CFC (pre- *vs.* post-US) and did not differ between the viral groups. During the Recent extinction session, freezing decreased in both groups, and no significant effect of viral manipulation was observed. Consolidation of recent extinction memory was assessed 24 hours later in the same context (Test), and no differences in freezing levels were detected between hM4Di- and mCherry-expressing mice (Fig. 2C). In both groups, freezing during the Test was significantly reduced compared to the beginning of extinction (E5), with a comparable magnitude of change (Fig. 2D–E), indicating that chemogenetic inhibition of the MS during Recent extinction did not affect contextual fear recall or extinction memory consolidation.

During the Remote extinction session, mice in both groups also exhibited a significant reduction in freez-

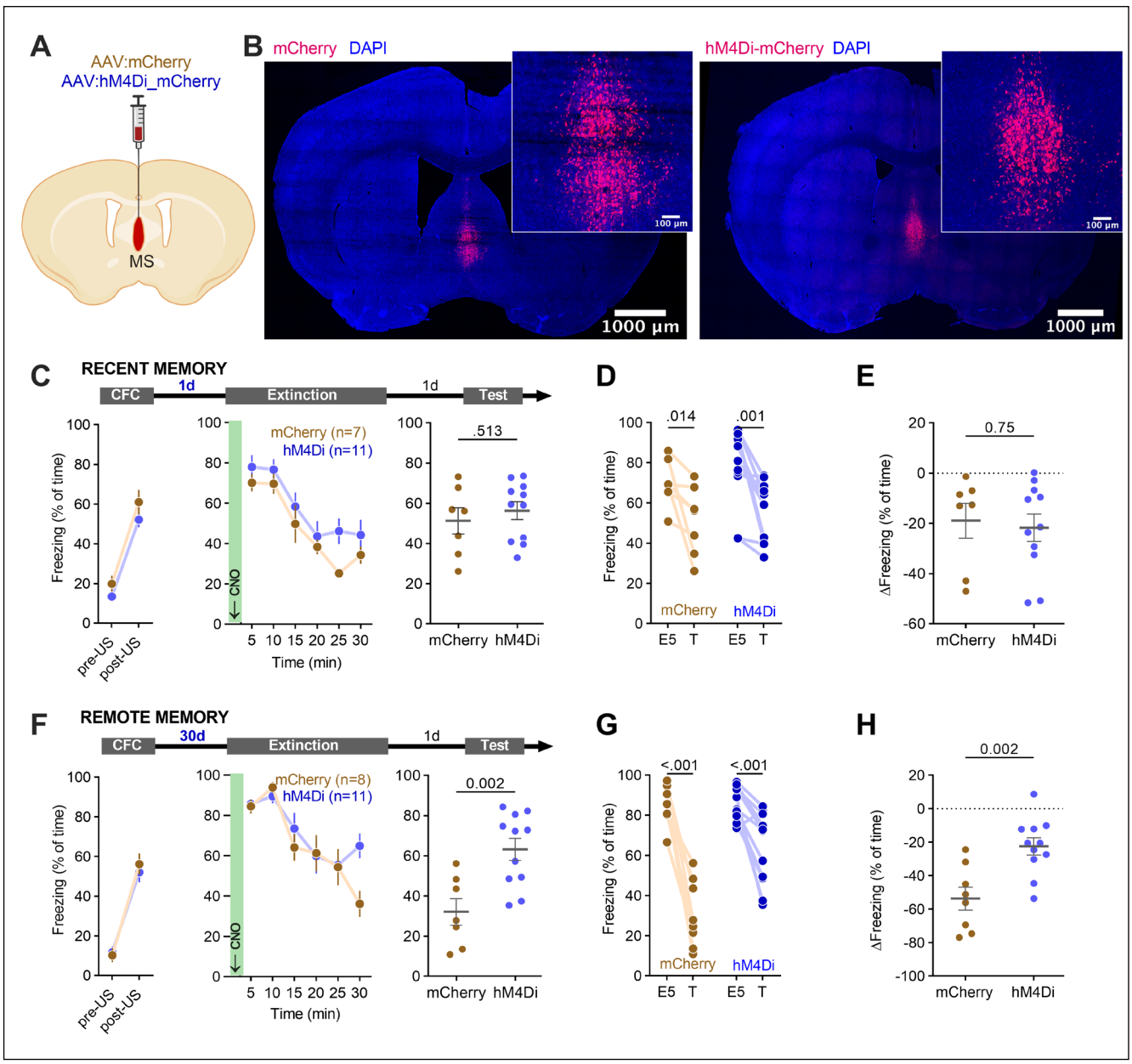


Fig. 2. MS regulates extinction of remote contextual fear memory. (A-B) Surgery schema and representative microphotographs of AAV: mCherry (mCherry) and AAV: hM4Di_mCherry (hM4Di) expression in MS. (C-E) Experimental timeline and summary of data for freezing levels during the extinction of recent contextual fear memory. After stereotactic injection of hM4Di (n=11) or mCherry (n=7) into MS, mice underwent CFC (CFC: RM ANOVA, effect of time: $F_{(1,13)}$=172, P<0.001; effect of virus: $F_{(1,13)}$=2.37, P=0.148; time × virus interaction: $F_{(1,13)}$=0.156, P=0.699), followed by recent fear memory extinction session 1 day later (Extinction: RM ANOVA, effect of time: $F_{(3.87,62.0)}$=26.3, P<0.001; effect of virus: $F_{(1,16)}$=1.93, P=0.184; time × virus interaction: $F_{(5,80)}$=0.689, P=0.634) and fear extinction test on the next day (Test: unpaired t-test: t(16)=0.669, P=0.513). Mice were injected with CNO (i.p., 3 mg/kg) 30 minutes prior to the extinction session. (D-E) Summary of data showing freezing levels during the first 5 minutes of the extinction session (E5) and test (T) (RM ANOVA, effect of time: $F_{(1,16)}$=21.5, P<0.001; effect of virus: $F_{(1,16)}$=0.968, P=0.340; time × genotype interaction: $F_{(1,16)}$=0.101, P=0.755), and the change of freezing frequency during T as compared to E5 (unpaired t-test: t(16)=0.669, P=0.513). (F-H) Experimental timeline and summary of data for freezing levels during the extinction of remote contextual fear memory. After stereotactic injection of hM4Di (n=11) or mCherry (n=8) into MS, mice underwent CFC (CFC: RM ANOVA, effect of time: $F_{(1,17)}$=193, P<0.001; effect of virus: $F_{(1,17)}$=0.061, P=0.807; time × virus interaction: $F_{(1,17)}$=0.864, P=0.366), remote fear memory extinction session 30 days later (Extinction: RM ANOVA, effect of time: $F_{(2.83,48.0)}$=18.3, P<0.001; effect of virus: $F_{(1,17)}$=0.819, P=0.378; time × virus interaction: $F_{(5,85)}$=2.42, P=0.042) and fear extinction test on the next day (Test: unpaired t-test: t(16)=3.585, P=0.002). (G-H) Summary of data showing freezing levels during the first 5 minutes of the extinction session (E5) and test (T) (RM ANOVA, effect of time: $F_{(1,17)}$=82.6, P<0.001; effect of virus: $F_{(1,17)}$=11.7, P=0.003; time × virus interaction: $F_{(1,17)}$=13.9, P=0.002), and the change of freezing frequency during T as compared to E5 (unpaired t-test: t(17)=3.728, P=0.002).

ing, indicating successful within-session extinction, and no immediate effect of viral manipulation was detected. However, during the extinction memory test, hM4Di-expressing mice displayed significantly higher freezing levels than controls (Fig. 2F). Further analysis revealed that although freezing during the Test was reduced relative to E5 in both groups, this reduction was significantly greater in mCherry control mice than in hM4Di mice (Fig. 2G–H). Thus, chemogenetic inhibition of the MS during Remote, but not Recent, extinction impaired consolidation of contextual fear extinction memory.

## Contribution of RE to extinction of contextual fear memory

Activity of RE is synchronized with freezing bouts (Totty et al., 2023), suggesting that activity patterns in the RE are related to suppression of fear responses. As c-Fos mapping identified correlation of MS and RE activity in the following experiment we tested the role of RE in extinction of recent and remote memory. To this end C57BL/6J mice were injected into RE with AAVs encoding hM4Di or mCherry (Fig. 3A-B). Three (for recent groups) or one (for remote groups) week post-surgery and viral transduction mice underwent CFC, followed by a recent or remote contextual fear extinction session (1 or 30 days post CFC, respectively). Mice were injected with CNO (i.p., 3 mg/ kg) prior to the Extinction. The freezing levels increased within the conditioning session (pre- *vs.* post-US) and did not differ between the drug groups. During the Recent extinction session, the hM4Di mice had overall higher freezing levels as compared to the mCherry animals. Consolidation of recent fear extinction memory was tested 24 hours after the Extinction session in the same context (Test). Mice from the hM4Di group tend to have lower levels of freezing as compared to the mCherry animals, but the difference was not statistically significant (Fig. 3C). Further analysis of the behavioral data revealed that mice in both groups similarly decreased freezing levels in the Test, as compared to E5 (Fig. 3D-E).

During the Remote extinction session, mice in both experimental groups significantly decreased freezing levels indicating successful within session fear extinction; however, hM4Di mice again showed slightly higher overall freezing levels. Notably, when the fear extinction memory was tested, the hM4Di animals demonstrated higher levels of freezing (Fig. 3F). Further analysis of the behavioral data revealed that although both hM4Di and mCherry mice had lower levels of freezing during the Test as compared to E5, the change was larger in the control group (Fig. 3G-H). Hence, chemogenetic inhibition of RE during the Remote, but not Recent, extinction session impaired consolidation of fear extinction memory.

## RE→MS projections

As both RE and MS contribute to extinction of remote fear memory and the activity of these regions correlates following remote extinction, we hypothesized that projections between RE and MS contribute to extinction of remote contextual fear memory. As the data about the direct projections between RE and MS (RE→MS) are controversial (McKenna & Vertes, 2004; Vertes et al., 2006; Cassel et al., 2013, 2021; Scheel et al., 2020), we first tested the presence of such projections using Ai14 mice that express Cre-dependent red fluorescent protein, tdTomato. Ai14 mice were stereotactically injected into MS with a retrograde AAV (rAAV) encoding Cre recombinase allowing for transduction of axons terminating in MS and tdTomato expression in the cell bodies (Madisen et al., 2010; Zingg et al., 2017) (Fig. 4A-B). tdTomato-positive cells were found mostly in the rostral RE (Bregma: -0.40 to -1.00 mm), and much less in the caudal part (Bregma: -1.00 to -1.88 mm) (Fig. 4C). We also observed tdTomato-positive cells in the brain regions well known to innervate MS, such as dCA1 and BLA (Liu et al., 2021; Tao et al., 2021) (Fig. 4C). Moreover, injection of AAV1 encoding mScarlet into RE allowed visualization of scarce projections in MS (Supplementary Fig. 3), supporting the notion that MS is innervated by RE.

## Activation of RE$^{\neg MS}$ neurons during fear extinction

To determine whether MS-projecting RE neurons (RE$^{\neg MS}$) are activated during contextual fear extinction, C57BL/6J mice were stereotactically injected into the MS with rAAV encoding GFP. This approach enabled GFP expression specifically in neurons projecting to the MS, including RE$^{\neg MS}$ neurons (Fig. 5A). One or three weeks after surgery, mice underwent CFC, followed by recent or remote fear extinction conducted 1 or 28 days after CFC, respectively. Mice were perfused 70 minutes after the extinction session, and their brains were processed for c-Fos analysis. Naive mice were included as controls. Confocal analysis of immunostained brain sections identified c-Fos$^+$ cells, GFP-positive RE neurons (GFP$^+$; RE$^{\neg MS}$), and double-positive neurons (c-Fos$^+$/GFP$^+$), representing activated RE neurons projecting to the MS. We confirmed

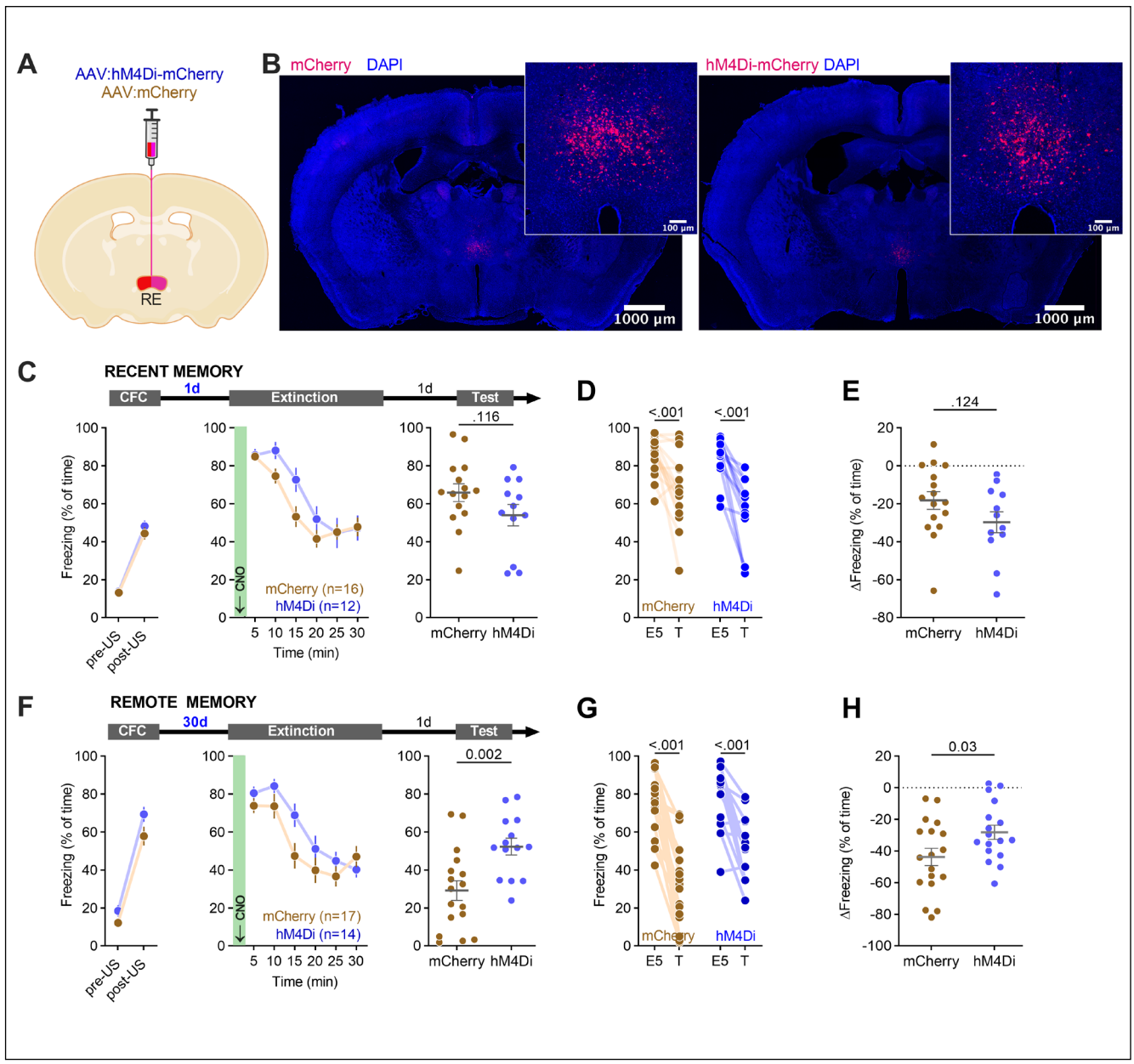


Fig. 3. RE regulates extinction of remote contextual fear memory. (A-B) Surgery schema and representative microphotographs of AAV: hM4Di_mCherry (hM4Di) and AAV: mCherry (mCherry) expression in RE. (C-E) Experimental timeline and summary of data for freezing levels during the extinction of recent contextual fear memory. After stereotactic injection of hM4Di (n=12) or mCherry (n=16) into RE, mice underwent CFC (CFC: RM ANOVA, effect of time: $F_{(1,32)}$=509, P<0.001; effect of virus: $F_{(1,32)}$=0.026, P=0.871; time × virus interaction: $F_{(1,32)}$=0.018, P=0.892), followed by recent fear memory extinction session 1 day later (Extinction: RM ANOVA, effect of time: $F_{(3.28,78.8)}$=39.2, P<0.001; effect of virus: $F_{(1, 24)}$=2.05, P=0.165; time × virus interaction: $F_{(5,120)}$=2.16, P=0.063) and fear extinction test on the next day (Test: unpaired t-test: t(25)=1.63, P=0.116). Mice were injected with CNO (i.p., 3 mg/kg) 30 minutes prior to the extinction session. (D-E) Summary of data showing freezing levels during the first 5 minutes of the extinction session (E5) and test (T) (RM ANOVA, effect of time: $F_{(1,26)}$=43.9, P<0.001; effect of virus: $F_{(1, 26)}$=2.69, P=0.113; time × genotype interaction: $F_{(1,26)}$=2.53, P=0.124), and the change of freezing frequency during T as compared to E5 (unpaired t-test: t(26)=1.59, P=0.124). (F-H) Experimental timeline and summary of data for freezing levels during the extinction of remote contextual fear memory. After stereotactic injection of hM4Di (n=14) or mCherry (n=17) into RE, mice underwent CFC (CFC: RM ANOVA, effect of time: $F_{(1,31)}$=443.8, P<0.001; effect of virus: $F_{(1,31)}$=3.680, P=006; time × virus interaction: $F_{(1,31)}$=1.226, P=0.28), remote fear memory extinction session 30 days later (Extinction: RM ANOVA, effect of time: $F_{(3.97,115)}$=27.8, P<0.001; effect of virus: $F_{(1,29)}$=2.64, P=0.115; time × virus interaction: $F_{(5,145)}$=1.98, P=0.086) and fear extinction test on the next day (Test: unpaired t-test: t(29)=3.337, P=0.002). (G-H) Summary of data showing freezing levels during the first 5 minutes of the extinction session (E5) and test (T) (RM ANOVA, effect of time: $F_{(1,31)}$=88.3, P<0.001; effect of virus: $F_{(1, 31)}$=5.09, P=0.031; time × virus interaction: $F_{(1,31)}$=5.66, P=0.024), and the change of freezing frequency during T as compared to E5 (unpaired t-test: t(33)=2.201, P=0.03).

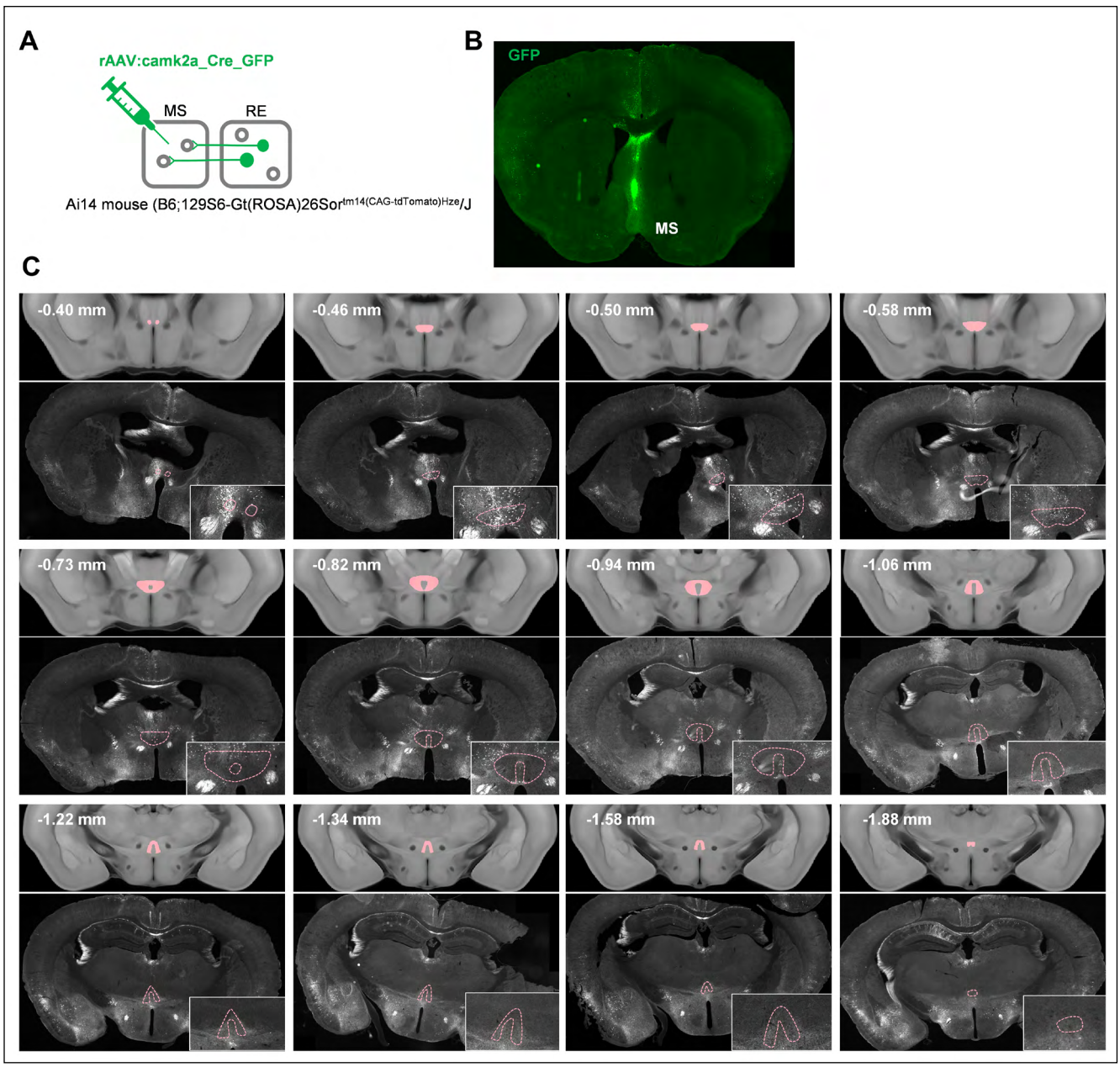


Fig. 4. Identification of anatomical projections from anterior RE to MS. Ai14 mice (with Cre-dependent tdTomato) (n=3) were injected into MS with rAAV: Cre_GFP resulting in tdTomato expression in neurons projecting to MS. (A-B) Surgery schema and representative microphotographs of rAAV: Cre_GFP expression in MS. (C) Microphotographs of tdTomato expression in Ai14 mouse (bottom) along with microphotographs of Allen mouse brain atlas (top). RE is marked in pink. Brain coordinates according to Bregma are indicated for each set of pictures.

that RE$^{\rightarrow MS}$ neurons were more abundant in the rostral, as compared to caudal, RE (Bregma > –1 *vs.* <-1 mm) (Fig. 5C). In the rostral RE, total c-Fos expression was increased in the recent and remote extinction groups compared with controls (Fig. 5D). No effect of the training on c-Fos levels was observed in the caudal RE. The density of c-Fos$^{+}$/GFP$^{+}$ neurons was also higher in the rostral RE in both extinction groups relative to controls (Fig. 5E). In contrast, in the caudal RE, the frequency of c-Fos$^{+}$/GFP$^{+}$ neurons was selectively increased in the remote extinction group compared with both controls and the recent group, indicating that rostral RE$^{\rightarrow MS}$ neurons are activated both by recent and remote fear extinction, caudal RE$^{\rightarrow MS}$ neurons are preferentially activated during extinction of remote contextual fear.

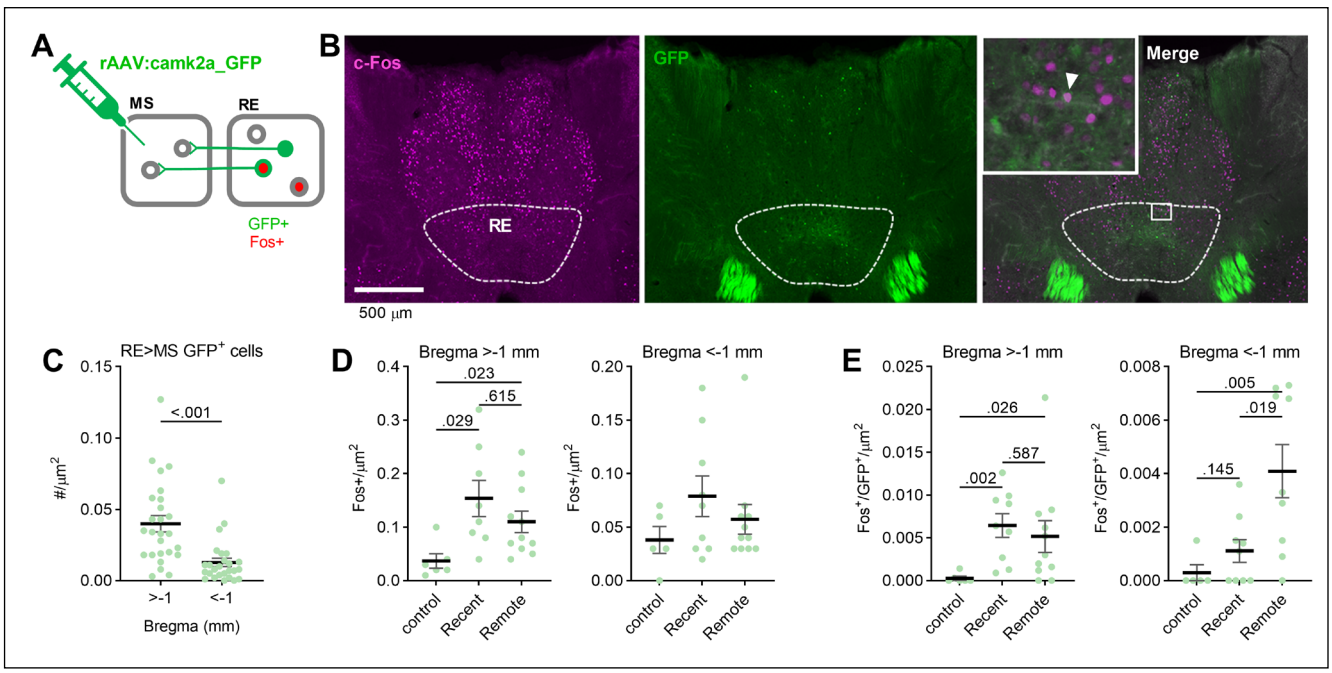


Fig. 5. Extinction of remote fear memory activates caudal RE$^{\rightarrow MS}$. (A) Mice had rAVV: *camk2a*_GFP stereotactically injected into MS and underwent CFC followed by extinction of recent (n=8) or remote (n=10) fear memory. Naive animals (n=6) were used as controls. GFP and c-Fos expression was analysed in the rostral and caudal RE (Bregma >-1 mm and <-1 mm). (B) Exemplary microphotographs of c-Fos immunostaining, GFP expression and their colocalisation in the rostral RE. White arrow in the inset indicates a double-positive cell. (C-E) Summary of data for GFP$^+$ cells density in the rostral and caudal RE (Mann-Whitney U=112). (D) Summary of data for c-Fos$^+$ cells density in the rostral (Welch's ANOVA test, $F_{(2,13.6)}$=7.83, P=0.005) and caudal RE ($F_{(2,13,4)}$=1.62, P=0.234). (E) Summary of data for c-Fos$^+$/GFP$^+$ cells density in the rostral ($F_{(2,12.3)}$=12.2, P=0.001) and caudal RE ($F_{(2,13.0)}$=6.8, P =0 0.009).

## Contribution of RE→MS projections to extinction of contextual fear memory

Next, to test whether RE→MS pathway affects extinction of contextual fear memory, C57BL/6J mice were stereotactically injected into RE with AAV encoding double-floxed inverted open reading frame (DIO) of hM4Di and mCherry, or just mCherry, under *camk2a* promoter (AAV: DIO_hM4Di_mCherry or AAV: DIO_mCherry), and into MS with rAAV encoding improved Cre recombinase (iCre) with eGFP under *camk2a* promoter (rAAV: iCre_eGFP). This combinatorial manipulation allowed for hM4Di expression specifically in RE$^{\rightarrow MS}$ (Fig. 6A-B). Three weeks post-surgery and viral transduction, mice underwent CFC, followed by a Recent or Remote contextual fear extinction session. Mice were injected with CNO (i.p., 3 mg/ kg) 30 minutes prior to the Extinction. The freezing levels increased within the CFC session (pre- *vs.* post-US) in all experimental groups and did not differ between the virus groups. During the Recent Extinction session, the mice from two experimental groups had similar freezing levels at the beginning of the session and decreased freezing during the session, indicating no impairment of fear memory recall and successful within-session fear extinction. Consolidation of long-term fear extinction memory was tested 24 hours after the Extinction session in the same context (Test) (Fig. 6C). Mice from two experimental groups had lower freezing levels during the Test as compared to E5, indicating successful consolidation of fear extinction memory (Fig. 6D). No difference in freezing levels were observed between the experimental groups (Fig. 6E).

During the Remote extinction session, mice in both experimental groups significantly decreased freezing levels indicating successful within session fear extinction. The hM4Di groups showed, however, overall higher freezing levels. Moreover, the hM4Di animals also demonstrated higher levels of freezing when the fear extinction memory was tested (Fig. 6F). Further analysis of the behavioral data revealed that although both hM4Di and mCherry mice had lower levels of freezing during the Test as compared to E5, the change was significantly greater in the control group (Fig. 6G-H). Hence, chemogenetic inhibition of RE→MS projection during the Remote, but not Recent, extinction session impaired consolidation of fear extinction memory.

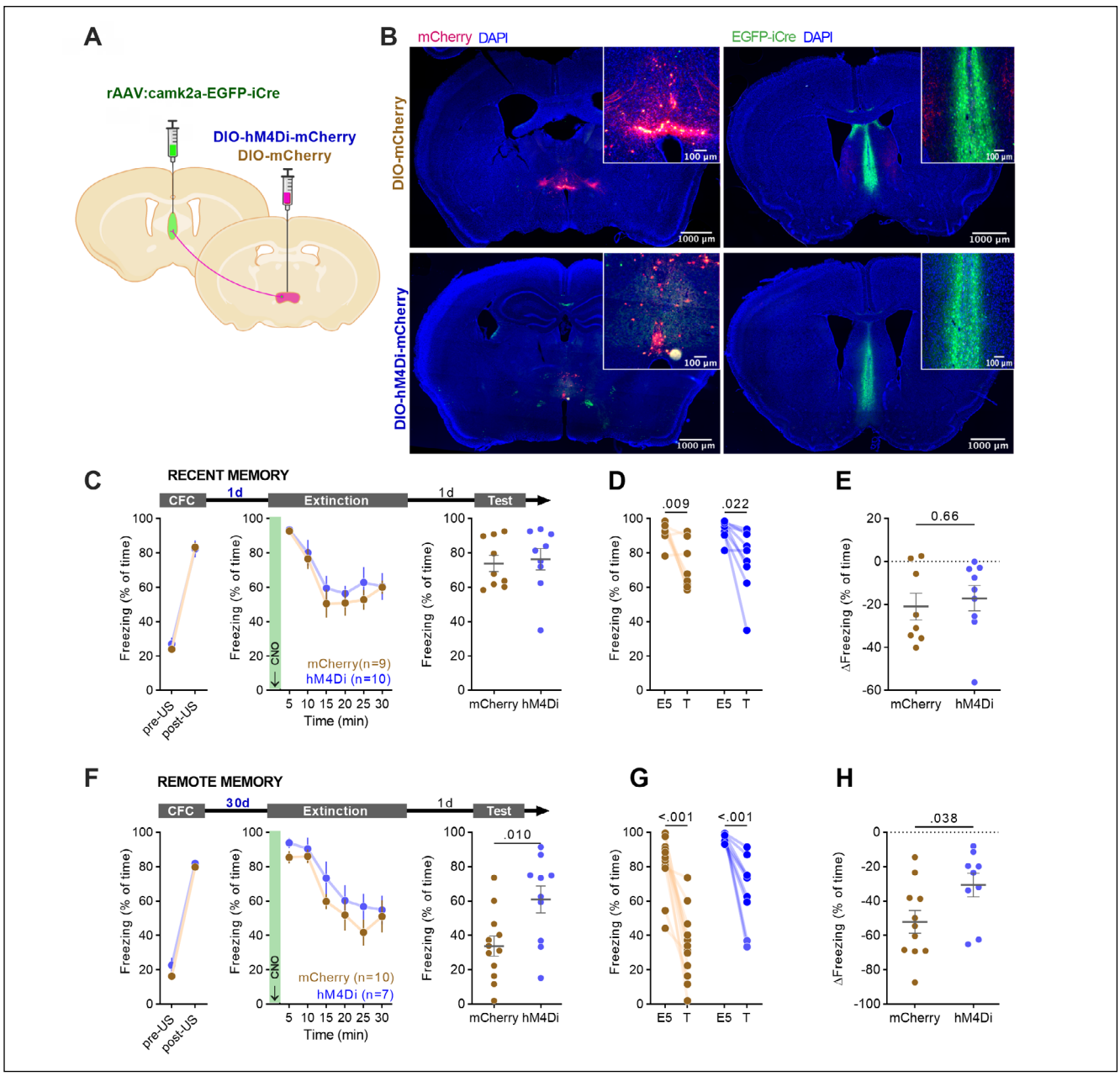


Fig. 6. RE→MS projections regulate consolidation of remote contextual fear extinction memory. AAV: DIO-hM4Di-mCherry (hM4Di) or control virus AAV: αCaMKII-DIO-mCherry (mCherry) were bilaterally injected to RE, while rAAV: iCre_eGFP-αCaMKII (eGFP) to MS of C57BL/6J male mice. (A-B) Surgery schema and representative microphotographs of hM4Di and mCherry in RE, and eGFP expression in MS. (C-E) Experimental timeline and summary of data for freezing levels during the extinction of recent contextual fear memory. After stereotactic injection of hM4Di (n=10) or mCherry (n=9) into RE and eGFP into MS, mice underwent CFC (CFC: RM ANOVA, effect of time: $F_{(1,15)}$=414, P<0.001; effect of virus: $F_{(1,15)}$=0.056, P=0.82), followed by recent fear memory extinction session 1 day later (Extinction: RM ANOVA, effect of time: $F_{(1,15)}$=19.68, P<0.001; effect of virus: $F_{(1,15)}$=0.648, P=0.43) and fear extinction test on the next day (Test: unpaired t-test: t(16)=0.318, P=0.75). Mice were injected with CNO (i.p., 3 mg/kg) 30 minutes prior to the extinction session. (D-E) Summary of data showing freezing levels during the first 5 minutes of the extinction session (E5) and test (T) (RM ANOVA, effect of time: $F_{(1,15)}$=19.7, P<0.001; effect of virus: $F_{(1, 15)}$=0.405, P=0.534; time × virus interaction: $F_{(1,15)}$=0.201, P=0.660), and the change of freezing frequency during T as compared to E5 (unpaired t-test: t(15)=0.448, P=0.66). (F-H) Experimental timeline and summary of data for freezing levels during the extinction of remote contextual fear memory. After stereotactic injection of hM4Di (n=7) or mCherry (n=10) into MS, mice underwent CFC (CFC: RM ANOVA, effect of time: $F_{(1,11)}$=201.3, P<0.001; effect of virus: $F_{(1,11)}$=0.0190, P=0.89; time × virus interaction: $F_{(1,11)}$=0.0057, P=0.94), remote fear memory extinction session 30 days later (Extinction: RM ANOVA, effect of time: $F_{(5,65)}$=13.60, P<0.001; effect of virus: $F_{(1,13)}$=5.402, P=0.04; time × virus interaction: $F_{(5,65)}$=1.465, P=0.21) and fear extinction test on the next day (Test: unpaired t-test: t(12)=2.88 P=0.01). (G-H) Summary of data showing freezing levels during the first 5 minutes of the extinction session (E5) and test (T) (RM ANOVA, effect of time: $F_{(1,13)}$=52.1, P<0.001; effect of virus: $F_{(1,13)}$=2.33, P=0.151; time × virus interaction: $F_{(1,13)}$=3.77, P=0.074), and the change of freezing frequency during T as compared to E5 (unpaired t-test: t(11)=3.39, P=0.006).

## Role of αCaMKII autophosphorylation in extinction of recent and remote contextual fear memory

CaMKII is one of the key synaptic molecules that contributes not only to formation and updating of recent contextual memories but also to systems consolidation of remote memories (Giese et al., 1998; Frankland et al., 2001; Kimura et al., 2008; Radwanska et al., 2011, 2015; Wheeler et al., 2013). Here, we tested the effect of heterozygous T286A mutation ($T286A^{+/-}$) of αCaMKII, that affects enzyme autophosphorylation and $Ca^{2+}$-independent activity (Giese et al., 1998), on extinction of recent and remote contextual fear memory as well as extinction-induced neuronal activity. To this end $T286A^{+/-}$ mice and their wild-type (WT) littermates underwent CFC and extinction of recent or remote fear memories. At the beginning of the CFC freezing levels were low but increased during the training in both genotypes. At the beginning of the Recent Extinction session freezing levels were high in both experimental groups indicating contextual fear memory formation, and decreased within the session. Mice of both genotypes significantly decreased the frequency of freezing during the Test (T) as compared to the beginning of the Extinction session (E5) indicating formation of fear extinction memory. No significant differences in fear extinction memory was observed between the genotypes (Fig. 7A-C).

Next, we tested the effect of $T286A^{+/-}$ mutation on the extinction of remote contextual fear memory. As previously, at the beginning of the Extinction session freezing levels were high in both experimental groups, indicating contextual fear memory recall, and slightly decreased during the session. Fear extinction memory was tested on the next day. While WT mice significantly decreased the frequency of freezing during the Test as compared to E5 indicating formation of fear extinction memory, such an effect was not observed for $T286A^{+/-}$ mutants. The freezing levels of the heterozygotes during the Test did not significantly differ from the levels observed during E5, indicating no extinction of remote contextual fear memory (Fig. 7D-F). Hence higher levels of autophosphorylated αCaMKII are required for updating of remote *vs.* recent contextual fear memory.

## Neuronal correlates of remote contextual fear memory extinction

As $T286A^{+/-}$ mutant mice showed impaired extinction of remote contextual fear memory we assumed that this mouse model is an excellent tool to further study neuronal correlates of this phenomenon. To this end $T286A^{+/-}$ mutant mice underwent CFC and Extinction session 1 or 30 days after CFC (Recent and Remote groups, respectively). The animals were sacrificed 70 minutes after the Extinction sessions. In addition, we used 3 control groups: naive mice taken from home cages, 5US groups sacrificed 1 day after CFC without Extinction session, and context controls (Ctx) that were

Fig. 7. $T286A^{+/-}$ mutation impairs extinction of remote contextual fear memory and extinction-induced brain activity. (A-C) Experimental timeline and summary of data for freezing levels during the extinction of recent contextual fear memory. $T286A^{+/-}$ (n=6) and WT (n=5) mice underwent CFC (CFC: RM ANOVA, effect of time: $F_{(1,10)}$=236, P<0.001; effect of genotype: $F_{(1,10)}$=0.293, P=0.600; time × genotype interaction: $F_{(1,10)}$=2.20, P=0.169), followed by recent fear memory extinction session 1 day later (Extinction: RM ANOVA, effect of time: $F_{(1.24,11.2)}$=7.30, P=0.016; effect of genotype: $F_{(1,9)}$=1.25, P=0.292; time × genotype interaction: $F_{(3,27)}$=0.078, P=0.971) and fear extinction test on the next day (Test: unpaired t-test: t(10)=0.578, P=0.576). (B-C) Summary of data showing freezing levels during the first 5 minutes of the extinction session (E5) and test (T) (RM ANOVA, effect of time: $F_{(1,10)}$=25.33, P<0.001; effect of genotype: $F_{(1,10)}$=0.519, P=0.49; time × genotype interaction: $F_{(1,10)}$=1.728, P=0.22), and the change of freezing frequency during T as compared to E5 (unpaired t-test: t(10)=1.314, P=0.22). (D-F) Experimental timeline and summary of data for freezing levels during the extinction of remote contextual fear memory. $T286A^{+/-}$ (n=6) and WT (n=6) mice underwent CFC (CFC: RM ANOVA, effect of time: $F_{(1, 10)}$=186, P<0.001; effect of genotype: $F_{(1,10)}$=6.56, P=0.028; time × genotype interaction: $F_{(1,10)}$=0.143, P=0.713), remote fear memory extinction session 30 days later (Extinction: RM ANOVA, effect of time: $F_{(1.31,13.1)}$=2.06, P=0.173; effect of genotype: $F_{(1,10)}$=3.97, P=0.074; time × genotype interaction: $F_{(3,30)}$=0.170, P=0.916) and fear extinction test on the next day (Test: unpaired t-test: t(10)=3.271, P=0.008). (E-F) Summary of data showing freezing levels during the first 5 minutes of the extinction session (E5) and test (T) (RM ANOVA, effect of time: $F_{(1,10)}$=28.48. P<0.001; effect of genotype: $F_{(1,10)}$=21.81, P<0.001; time × genotype interaction: $F_{(1,10)}$=3.880, P=0.08), and the change of freezing frequency during T as compared to E5 (unpaired t-test: t(10)=2.01, P=0.036). (G). Fold change of the c-Fos signal density for T286A+/- mice, where the recent (Rec) and remote (Rem) extinction groups are compared to mice sacrificed 24 hours after CFC (5US) or to each other (n=6 mice per group, n=9-39 sections per region, per group). (H) Fold change of c-Fos signal density for T286A+/- mice as compared to WT animals. Naive, mice taken from home cages; Ctx, mice exposed twice to the novel context without US experience. See Supplementary Fig. 1 for the experimental groups description. (I, J) Significant change of the c-Fos signal density for T286A+/- mice (based on FDR results). (K, L) Significant correlation of c-Fos density signal for T286A+/- mice after Recent and Remote extinction (based on Spearman correlations). PrL, prelimbic cortex; IL, infralimbic cortex; CG, cingulate cortex; RSG, retrosplenial cortex, granular part; RSA, retrosplenial cortex, agranular part; V1, primary visual cortex; ENT, entorhinal cortex; LS, lateral septum; MS, medial septum; AD, anterodorsal nucleus of thalamus; AV, anteroventral nucleus of thalamus; AM, anteromedial nucleus of thalamus; LD, laterodorsal nucleus of thalamus; RE, nucleus reuniens; CM, centromedial nucleus of thalamus; MD, mediodorsal nucleus of thalamus; PV, paraventricular nucleus of thalamus; CA1, dorsal hippocampus, CA1 area; CA3, dorsal hippocampus, CA3 area; DG, dentate gyrus; BLA, basolateral nucleus of the amygdala; LA, lateral nucleus of the amygdala; CeA, central nucleus of the amygdala, capsular and lateral divisions; CeM, central nucleus of the amygdala, centromedial division.

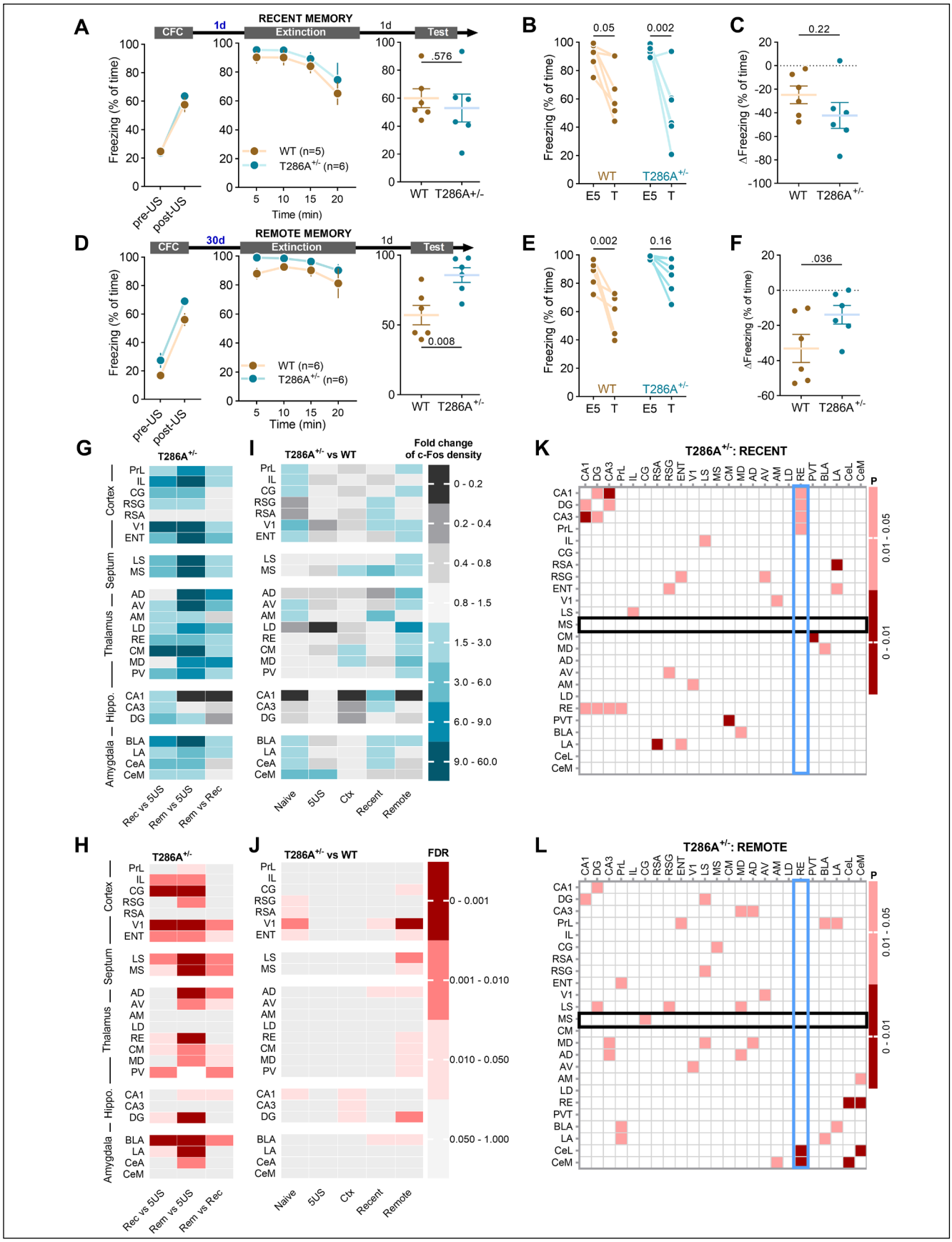
A
RECENT MEMORY
CFC
1d
Extinction
1d
Test
Freezing (% of time)
pre-US
post-US
WT (n=5)
T286A+/- (n=6)
Time (min)
.576
WT T286A+/-
B
0.05
0.002
WT
T286A+/-
E5 T E5 T
C
0.22
ΔFreezing (% of time)
WT T286A+/-
D
REMOTE MEMORY
CFC
30d
Extinction
1d
Test
WT (n=6)
T286A+/- (n=6)
0.008
E
0.002
0.16
F
.036
G
T286A+/-
Cortex
Septum
Thalamus
Hippo.
Amygdala
PrL IL CG RSG RSA V1 ENT
LS MS
AD AV AM LD RE CM MD PV
CA1 CA3 DG
BLA LA CeA CeM
Rec vs 5US
Rem vs 5US
Rem vs Rec
I
T286A+/- vs WT
Fold change of c-Fos density
0 - 0.2
0.2 - 0.4
0.4 - 0.8
0.8 - 1.5
1.5 - 3.0
3.0 - 6.0
6.0 - 9.0
9.0 - 60.0
Naive 5US Ctx Recent Remote
K
T286A+/-: RECENT
CA1 DG CA3 PrL IL CG RSA RSG ENT V1 LS MS CM MD AD AV AM LD RE PVT BLA LA CeL CeM
P
0.01 - 0.05
0 - 0.01
H
T286A+/-
FDR
0 - 0.001
0.001 - 0.010
0.010 - 0.050
0.050 - 1.000
J
T286A+/- vs WT
L
T286A+/-: REMOTE

exposed to the experimental context twice but never received USs and were sacrificed 70 minutes after the last context exposure (Supplementary Fig. 1A). Mice brains were sliced and used for immunofluorescent staining to detect c-Fos. c-Fos expression was analyzed in 23 brain regions of the dorsal hippocampus, amygdala, cortex, thalamus, and septum and compared with data for WT mice (Fig. 1). c-Fos data shown on Fig. 1 and Fig. 7 were processed in parallel and come from WT and T286A$^{+/-}$ littermates.

Overall, in T286A$^{+/-}$ mutant mice, as in WT animals (Fig. 1D-G), we observed a significant elevation of c-Fos levels in many brain regions following Recent and Remote extinction, as compared to 5US animals of the same genotype (Fig. 7G-H). The changes were, however, more pronounced after Remote as compared to Recent extinction - a significant increase in c-Fos levels was found in 12 regions of T286A$^{+/-}$ mice after Recent, and 17 after Remote extinction (Fig. 7G-H). In 10 regions (V1, ENT, LS, MS, AD, AV, CM, MD, PV, BLA) c-Fos levels were significantly higher in Remote *vs.* Recent groups. In addition, c-Fos levels were significantly lower in CA1 in the Remote *vs.* Recent T286A$^{+/-}$ group. Furthermore, when we compared c-Fos levels between WT and T286A$^{+/-}$ mutant mice the biggest differences were observed between the Remote extinction groups (Fig. 7I-J) – in 9 regions T286A$^{+/-}$ mutant mice had higher expression of c-Fos as compared to WT animals (CG, V1, Ent, LS, MS, AD, RE, CM and BLA), and c-Fos expression was lower in the mutants in DG. Furthermore, c-Fos levels were affected by the mutation in 5 regions in the naive groups, in 3 regions in Recent and Ctx groups and no significant differences were observed between the genotypes in 5US groups. Finally, we observed in T286A$^{+/-}$ mice an altered pattern of activity correlation after Recent and Remote extinction, as compared to WT mice (Fig. 1F-G), with decreased correlation of MS with RE in particular (Fig. 7K-L). Hence, elevated c-Fos levels in the cortex, septum, thalamus and amygdala, reduced c-Fos in the hippocampus and altered patterns of correlated activity are the neural hallmarks of impaired extinction of remote contextual fear memory in T286A$^{+/-}$ mutant mice. This observation suggests that αCaMKII activity in these regions contributes to systems consolidation and updating of the remote memory engram.

## DISCUSSION

The current study identifies neuronal networks involved in the extinction of remote contextual fear memory. In particular, we characterize the role of RE, MS, and RE→MS projections in the extinction of contextual fear memory as the memories age.

In our experiments, we evaluated extinction of contextual fear memory at both short and long delays after training. We found that in the wild-type (WT) animals functional networks differed at these two time-points, consistent with the idea that memory organization changes as a function of memory age, a process known as systems consolidation (Frankland & Bontempi, 2005). One prominent model of systems consolidation (Squire & Alvarez, 1995) proposes that memories are initially encoded in hippocampal-cortical networks, and that reactivation of these networks then leads to the incremental strengthening of inter-cortical connectivity, and an emergent role for cortical regions in memory expression coupled with disengagement of the hippocampus. In agreement with this model we see increased activity of the cortex (RSC and V1) in the remote time point. Furthermore, we see increased engagement of the septum (MS), thalamus (PV) and amygdala (BLA and LA) supporting the contribution of these regions in systems consolidation (Silva et al., 2021; Wheeler et al., 2013). However, we do not see significant change in the hippocampus engagement with time, possibly indicating differences between the contribution of this region in contextual fear memory formation, recall and extinction as the memory age. Interestingly, the role of some hotspots, including BLA, RSC, PV and PV→CeA projections, in remote memory processing has been already validated (Corcoran et al., 2011; Do-Monte et al., 2015; Silva et al., 2021).

Overall, our data indicates that extinction of remote memory engages more brain regions than recent memory. Interestingly, although previous studies linked broader memory networks with higher stabilization of remote memory (Milekic & Alberini, 2002; Frankland et al., 2006; Wheeler et al., 2013), in our experiments extinction of remote memory was more efficient. A remote extinction session resulted in WT mice in a reduction of freezing by 40-50% during the extinction test as compared to the beginning of the extinction session, while the recent extinction session reduced freezing by 20% measured during the test. Hence, increased stabilization of memories with time may be specific for traumatic and pathologic memories (Costanzi et al., 2011; Kearns et al., 2012), while in case of physiologic process extinction of remote fear memory may be enhanced by natural forgetting of aversive experience. Enhanced extinction observed in our model in the remote time point may reflect the fact that such a session engages more brain regions, hence, more efficiently remodels memory networks.

While correspondence between the predictions derived from the c-Fos analysis and these published

findings provides some validation of our approach, perhaps greater value lies in using this approach for the identification of novel, candidate brain regions. In this regard, it is interesting that both septal (MS and LS) and thalamic (RE, CM, AD) regions were identified. These regions, by virtue of their widespread connectivity with both the hippocampus and neocortex, are ideally positioned to influence network function. In particular, thalamic regions strongly influence cortical activity and therefore may play central roles in coordinating memory retrieval and extinction.

Several reports demonstrate the involvement of MS in extinction of fear memory (Calandreau et al., 2007; Knox et al., 2016; Xiao et al., 2018). In conjunction with anatomical data indicating dense connections of MS with the hippocampus (Amaral & Kurz, 1985; Nyakas et al., 1987; Khakpai et al., 2013; Müller & Remy, 2018) and the medial prefrontal cortex (Unal et al., 2015), the above observations suggest the involvement of MS in processing spatial information related to environmental threats. In particular, cholinergic neurons of MS regulate the extinction of recent contextual fear memory when extinction training consists of seven sessions conducted over seven days (Tronson et al., 2009). Lesions of MS and the adjacent nucleus of the diagonal band of Broca also led to impaired extinction of early fear memory dependent on auditory stimuli in rats (Knox & Keller, 2016). Here, we observed that c-Fos protein levels in MS are higher after the remote extinction session than after the recent extinction. Moreover, we did not observe a disruption of the extinction with chemogenetic inhibition of MS during the recent extinction session. However, we noticed that chemogenetic inactivation of MS during the remote extinction session impaired formation of the fear extinction memory. Thus, the changes in c-Fos expression and the results of chemogenetic manipulations are consistent and suggest that the involvement of MS in fear memory extinction changes as the memory age. These observations, however, seem to contradict the literature data cited above (Tronson et al., 2009). Possible reasons for this discrepancy may include differences in the conditioning and fear memory extinction protocols, as well as in the method and extent of MS neuron inactivation. Although Tronson et al. (2009) observed impaired recent fear memory extinction in mice with MS lesions compared to the control animals, these differences were only evident on the fourth day of extinction training. This observation is similar to the results of our experiment. Interestingly, this difference probably does not depend on the length of the extinction session (3 min in Tronson et al. (2009) *vs.* 30 min here), as in the study by Knox and Keller (2016), which used long extinction training, a similar pattern of changes in behavior was observed as after 3-minute extinctions. Therefore, the time from the conditioning to the extinction session seems to be crucial for the involvement of MS in fear memory extinction.

Indeed, former studies demonstrated the role of the RE in fear memory encoding, retrieval, extinction and fear generalization (Xu & Sudhof, 2013; Vetere et al., 2017; Ramanathan et al., 2018; Ramanathan & Maren, 2019; Troyner & Bertoglio, 2021; Vasudevan et al., 2022). Specifically, it has been demonstrated that RE is involved in the extinction of recent contextual and auditory fear memory (Ramanathan et al., 2018; Ramanathan & Maren, 2019). Administration of muscimol into the RE before the recent extinction session impairs within-session fear extinction as well as fear extinction memory tested on the following day (Ramanathan et al., 2018; Ramanathan & Maren, 2019). Administration of muscimol into the RE shortly after extinction training or extinction reconsolidation does not result in differences in freezing levels during the extinction memory test (Vasudevan et al., 2022). In opposition to these findings our experiments indicate that the involvement of the RE in fear memory extinction depends on the length of the interval between training and extinction sessions. Chemogenetic inhibition of RE neurons during the extinction of recent contextual fear memory slightly increased freezing levels during the extinction session but did not affect the consolidation of extinction memory. Chemogenetic inhibition of RE neurons during the extinction of remote contextual fear memory impaired both within-session extinction and consolidation of extinction memory. Reminiscent of these observations, permanent lesion of the RE impaired remote, but not recent, contextual fear memory (Quet et al., 2020) and chemogenetic manipulation of RE bidirectionally affects extinction of the remote contextual fear memory (Silva et al., 2021). The discrepancy between our results and the work of Marren's group (Vasudevan et al., 2022) may stem from differences in methods used to inhibit RE activity as well as training protocol. In particular, muscimol used by Ramanathan and Maren (2019) stimulates inhibitory GABAA receptors and strongly inhibits neuronal activity. Whereas, stimulation of the inhibitory hM4Di receptor results in a decrease rather than complete inhibition of neuronal activity (Smith et al., 2016). Finally, in the former studies, as compared to our experiments, the authors used a weaker training protocol (3US *vs.* 5US) and extended extinction session (35 min *vs.* 30 min) that resulted in more efficient contextual fear extinction (to 50-60% *vs.* 20% freezing). Hence, high levels of freezing observed in our experiments in the control groups following a re-

cent extinction session could mask the effect of RE inhibition on contextual fear extinction. In summary, our experiments suggest that the role of RE in extinction of contextual fear memory increases with time. Moreover, the extinction of remote and recent fear memory possibly involves different populations of RE neurons. The later hypothesis should be, however, validated in the future experiments.

RE innervates many brain structures and is innervated by over 30 areas (Cassel et al., 2021). It also has about 11% bifurcating neurons, which innervate both the cingulate cortex and the medial part of the prefrontal cortex, as well as the insular cortex (Yanakieva et al., 2022). So far, the functionally best-understood neuronal circuit involving RE is the mPFC→RE→hippocampal axis. Both mPFC→RE and RE→CA1 projections mediate the fear extinction process (Ramanathan et al., 2018; Ratigan et al., 2023; Totty et al., 2023). It has been shown that inhibiting RE→CA1 projections during the recall of recent fear memory leads to impaired fear memory extinction in subsequent days (Ratigan et al., 2023). Furthermore, RE→BLA projection participates in the extinction of remote contextual fear memory (Silva et al., 2021). It has been shown that both the activity of excitatory RE→BLA projections and the activity of RE cells increase shortly before the end of the extinction episode. Moreover, chemogenetic inhibition of these projections during late fear extinction impairs the extinction of late fear memory. On the other hand, optogenetic stimulation of GABAergic or dopaminergic cells in the zone incerta (ZI)→RE neuronal pathway leads to enhanced extinction of early fear memory dependent on auditory stimuli (Venkataraman et al., 2021), revealing a complex role of RE in the neuronal circuits of fear extinction. Here, we demonstrate that rostral $RE^{\neg MS}$ neurons are activated during extinction of both recent and remote contextual fear memories, whereas caudal $RE^{\neg MS}$ neurons are selectively activated during extinction of remote memories. Moreover, chemogenetic inhibition of excitatory RE→MS projections during fear extinction impairs extinction of remote, but not recent, contextual fear memory. Together, these findings indicate that the contribution of $RE^{\neg MS}$ neurons to fear extinction increases as memories age. Considering the consequences of inhibiting RE→MS projections in the context of anatomical connections, it is worth mentioning that both these regions innervate the CA1 area of the hippocampus, which is involved in extinction of contextual fear memory (Phillips & LeDoux, 1992; Maren & Holt, 2000; Maren & Quirk, 2004; Bissiere et al., 2011; Ziółkowska et al., 2025). MS and RE synchronize theta rhythms in the hippocampus and influence local field potentials in the hippocampus→RE→mPFC circuit (King et al., 1998; Roy et al., 2017).

We show that αCaMKII autophosphorylation deficient heterozygous mice ($T286A^{+/-}$) have impaired extinction of remote memory while the extinction of recent contextual fear memory is spared. Accordingly, we use this model to look for neuronal correlates of remote memory extinction. Although previous studies showed that T286A mutation affects extinction of recent contextual fear memory (more training trials are required for efficient extinction) (Kimura et al., 2008; Radwanska et al., 2011, 2015), this is the first demonstration showing that αCaMKII autophosphorylation affects remote memory updating. This finding is reminiscent of former studies showing that $\alpha CaMKII^{+/-}$ mice show impairment of remote memory storage (Frankland et al., 2001; Wheeler et al., 2013). Impaired remote memory extinction in $T286A^{+/-}$ mice is accompanied with globally increased activity of the thalamus (RE, CM, AD), septum (LS and MS), cortex (CG, V1, ENT) and amygdala (BLA), decreased activity of the hippocampus (DG), as well as altered networks correlations. Hence, impaired fear memory extinction in heterozygous may result from aberrant connectivity of fear extinction network and impaired systems consolidation. It is also possible that the decreased function of the hippocampus in the mutants during the Remote extinction session reflects impaired recall and/or updating of contextual fear memory.

In summary, the results presented here reveal a new element of neuronal circuits responsible for the extinction of remote contextual fear memory and highlight the importance of thalamo-septal circuits and αCaMKII autophosphorylation in the systems consolidation of remote memories. However, the important limitation of our study is the fact that the experiments involving chemogenetic manipulations have been conducted only on male mice. As fear memory processing shows significant sex differences (Bauer, 2023; Keiser et al., 2017), the role of the identified pathway in fear extinction by females has to be verified in the future studies.

## ACKNOWLEDGMENTS

This work was supported by the National Science Center (Poland) [PRELUDIUM Grant No. 2019/35/N/NZ4/01910 to KFT; and MAESTRO grant No. 2020/38/A/NZ4/00483 to KR]. The project was carried out with the use of CePT infrastructure financed by the European Union - The European Regional Development Fund within the Operational Program "Innovative economy" for 2007-2013.

# REFERENCES


Amaral, D. G., & Kurz, J. (1985). An analysis of the origins of the cholinergic and noncholinergic septal projections to the hippocampal formation of the rat. *The Journal of Comparative Neurology*, *240*(1), 37–59. https://doi.org/10.1002/cne.902400104

Bauer, E. P. (2023). Sex differences in fear responses: Neural circuits. *Neuropharmacology*, *222*, 109298. https://doi.org/10.1016/j.neuropharm.2022.109298

Bissiere, S., Zelikowsky, M., Ponnusamy, R., Jacobs, N. S., Blair, H. T., & Fanselow, M. S. (2011). Electrical synapses control hippocampal contributions to fear learning and memory. *Science (New York, N.Y.)*, *331*(6013), 87–91. https://doi.org/10.1126/science.1193785

Buzsáki, G. (1996). The hippocampo-neocortical dialogue. *Cerebral Cortex (New York, N.Y.: 1991)*, *6*(2), 81–92. https://doi.org/10.1093/cercor/6.2.81

Calandreau, L., Jaffard, R., & Desmedt, A. (2007). Dissociated roles for the lateral and medial septum in elemental and contextual fear conditioning. *Learning & memory (Cold Spring Harbor, N.Y.)*, *14*(6), 422–429. https://doi.org/10.1101/lm.531407

Cassel, J.-C., Ferraris, M., Quilichini, P., Cholvin, T., Boch, L., Stephan, A., & Pereira de Vasconcelos, A. (2021). The reuniens and rhomboid nuclei of the thalamus: A crossroads for cognition-relevant information processing? *Neuroscience and Biobehavioral Reviews*, *126*, 338–360. https://doi.org/10.1016/j.neubiorev.2021.03.023

Cassel, J.-C., Pereira de Vasconcelos, A., Loureiro, M., Cholvin, T., Dalrymple-Alford, J. C., & Vertes, R. P. (2013). The reuniens and rhomboid nuclei: Neuroanatomy, electrophysiological characteristics and behavioral implications. *Progress in Neurobiology*, *111*, 34–52. https://doi.org/10.1016/j.pneurobio.2013.08.006

Corcoran, K. A., Donnan, M. D., Tronson, N. C., Guzmán, Y. F., Gao, C., Jovasevic, V., Guedea, A. L., & Radulovic, J. (2011). NMDA Receptors in Retrosplenial Cortex Are Necessary for Retrieval of Recent and Remote Context Fear Memory. *Journal of Neuroscience*, *31*(32), 11655–11659. https://doi.org/10.1523/JNEUROSCI.2107-11.2011

Costanzi, M., Cannas, S., Saraulli, D., Rossi-Arnaud, C., & Cestari, V. (2011). Extinction after retrieval: Effects on the associative and nonassociative components of remote contextual fear memory. *Learning & Memory (Cold Spring Harbor, N.Y.)*, *18*(8), 508–518. https://doi.org/10.1101/lm.2175811

Do-Monte, F. H., Quiñones-Laracuente, K., & Quirk, G. J. (2015). A temporal shift in the circuits mediating retrieval of fear memory. *Nature*, *519*(7544), 460–463. https://doi.org/10.1038/nature14030

Feng, G., Mellor, R. H., Bernstein, M., Keller-Peck, C., Nguyen, Q. T., Wallace, M., Nerbonne, J. M., Lichtman, J. W., & Sanes, J. R. (2000). Imaging Neuronal Subsets in Transgenic Mice Expressing Multiple Spectral Variants of GFP. *Neuron*, *28*(1), 41–51. https://doi.org/10.1016/S0896-6273(00)00084-2

Frankland, P. W., & Bontempi, B. (2005). The organization of recent and remote memories. *Nature Reviews Neuroscience*, *6*(2), 119–130. https://doi.org/10.1038/nrn1607

Frankland, P. W., Ding, H.-K., Takahashi, E., Suzuki, A., Kida, S., & Silva, A. J. (2006). Stability of recent and remote contextual fear memory. *Learning & Memory*, *13*(4), 451–457. https://doi.org/10.1101/lm.183406

Frankland, P. W., O'Brien, C., Ohno, M., Kirkwood, A., & Silva, A. J. (2001). α-CaMKII-dependent plasticity in the cortex is required for permanent memory. *Nature*, *411*(6835), 309–313. https://doi.org/10.1038/35077089

Garfinkel, S. N., Abelson, J. L., King, A. P., Sripada, R. K., Wang, X., Gaines, L. M., & Liberzon, I. (2014). Impaired contextual modulation of memories in PTSD: An fMRI and psychophysiological study of extinction retention and fear renewal. *The Journal of Neuroscience: The Official Journal of the Society for Neuroscience*, *34*(40), 13435–13443. https://doi.org/10.1523/JNEUROSCI.4287-13.2014

Giese, K. P., Fedorov, N. B., Filipkowski, R. K., & Silva, A. J. (1998). Autophosphorylation at Thr286 of the alpha calcium-calmodulin kinase II in LTP and learning. *Science (New York, N.Y.)*, *279*(5352), 870–873. https://doi.org/10.1126/science.279.5352.870

Gomez, J. L., Bonaventura, J., Lesniak, W., Mathews, W. B., Sysa-Shah, P., Rodriguez, L. A., Ellis, R. J., Richie, C. T., Harvey, B. K., Dannals, R. F., Pomper, M. G., Bonci, A., & Michaelides, M. (2017). Chemogenetics revealed: DREADD occupancy and activation via converted clozapine. *Science*, *357*(6350), 503–507. https://doi.org/10.1126/science.aan2475

Grodin, E. N., Sussman, L., Sundby, K., Brennan, G. M., Diazgranados, N., Heilig, M., & Momenan, R. (2018). Neural Correlates of Compulsive Alcohol Seeking in Heavy Drinkers. *Biological Psychiatry. Cognitive Neuroscience and Neuroimaging*, *3*(12), 1022–1031. https://doi.org/10.1016/j.bpsc.2018.06.009

Irvine, E. E., Vernon, J., & Giese, K. P. (2005). αCaMKII autophosphorylation contributes to rapid learning but is not necessary for memory. *Nature Neuroscience*, *8*(4), 411–412. https://doi.org/10.1038/nn1431

Irvine, E. E., von Hertzen, L. S. J., Plattner, F., & Giese, K. P. (2006). αCaMKII autophosphorylation: A fast track to memory. *Trends in Neurosciences*, *29*(8), 459–465. https://doi.org/10.1016/j.tins.2006.06.009

Jendryka, M., Palchaudhuri, M., Ursu, D., van der Veen, B., Liss, B., Kätzel, D., Nissen, W., & Pekcec, A. (2019). Pharmacokinetic and pharmacodynamic actions of clozapine-N-oxide, clozapine, and compound 21 in DREADD-based chemogenetics in mice. *Scientific Reports*, *9*(1), 4522. https://doi.org/10.1038/s41598-019-41088-2

Ji, J., & Maren, S. (2007). Hippocampal involvement in contextual modulation of fear extinction. *Hippocampus*, *17*(9), 749–758. https://doi.org/10.1002/hipo.20331

Jiang, L., Kundu, S., Lederman, J. D., López-Hernández, G. Y., Ballinger, E. C., Wang, S., Talmage, D. A., & Role, L. W. (2016). Cholinergic Signaling Controls Conditioned Fear Behaviors and Enhances Plasticity of Cortical-Amygdala Circuits. *Neuron*, *90*(5), 1057–1070. https://doi.org/10.1016/j.neuron.2016.04.028

Kearns, M. C., Ressler, K. J., Zatzick, D., & Rothbaum, B. O. (2012). Early interventions for PTSD: A review. *Depression and Anxiety*, *29*(10), 833–842. https://doi.org/10.1002/da.21997

Keiser, A. A., Turnbull, L. M., Darian, M. A., Feldman, D. E., Song, I., & Tronson, N. C. (2017). Sex Differences in Context Fear Generalization and Recruitment of Hippocampus and Amygdala during Retrieval. *Neuropsychopharmacology: Official Publication of the American College of Neuropsychopharmacology*, *42*(2), 397–407. https://doi.org/10.1038/npp.2016.174

Khakpai, F., Nasehi, M., Haeri-Rohani, A., Eidi, A., & Zarrindast, M. R. (2013). Septo-hippocampo-septal loop and memory formation. *Basic and Clinical Neuroscience*, *4*(1), 5–23.

Kimura, R., Silva, A. J., & Ohno, M. (2008). Autophosphorylation of αCaMKII is differentially involved in new learning and unlearning mechanisms of memory extinction. *Learning & Memory*, *15*(11), 837–843. https://doi.org/10.1101/lm.1049608

King, C., Recce, M., & O'Keefe, J. (1998). The rhythmicity of cells of the medial septum/diagonal band of Broca in the awake freely moving rat: Relationships with behaviour and hippocampal theta. *The European Journal of Neuroscience*, *10*(2), 464–477. https://doi.org/10.1046/j.1460-9568.1998.00026.x

Kitamura, T., Ogawa, S. K., Roy, D. S., Okuyama, T., Morrissey, M. D., Smith, L. M., Redondo, R. L., & Tonegawa, S. (2017). Engrams and circuits crucial for systems consolidation of a memory. *Science*, *356*(6333), 73–78. https://doi.org/10.1126/science.aam6808

Knox, D. (2016). The Role Of Basal Forebrain Cholinergic Neurons In Fear and Extinction Memory. *Neurobiology of Learning and Memory*, *133*, 39–52. https://doi.org/10.1016/j.nlm.2016.06.001

Knox, D., & Keller, S. M. (2016). Cholinergic neuronal lesions in the medial septum and vertical limb of the diagonal bands of Broca induce contextual fear memory generalization and impair acquisition of fear extinction. *Hippocampus*. https://doi.org/10.1002/hipo.22553

Knox, D., Stanfield, B. R., Staib, J. M., David, N. P., Keller, S. M., & DePietro, T. (2016). Neural circuits via which single prolonged stress exposure leads

to fear extinction retention deficits. *Learning & Memory*, *23*(12), Article 12. https://doi.org/10.1101/lm.043141.116

Kügler, S., Kilic, E., & Bähr, M. (2003). Human synapsin 1 gene promoter confers highly neuron-specific long-term transgene expression from an adenoviral vector in the adult rat brain depending on the transduced area. *Gene Therapy*, *10*(4), 337–347. https://doi.org/10.1038/sj.gt.3301905

Lissek, S., Kaczkurkin, A. N., Rabin, S., Geraci, M., Pine, D. S., & Grillon, C. (2014). Generalized anxiety disorder is associated with overgeneralization of classically conditioned fear. *Biological Psychiatry*, *75*(11), 909–915. https://doi.org/10.1016/j.biopsych.2013.07.025

Liu, J., Hu, T., Zhang, M.-Q., Xu, C.-Y., Yuan, M.-Y., & Li, R.-X. (2021). Differential efferent projections of GABAergic neurons in the basolateral and central nucleus of amygdala in mice. *Neuroscience Letters*, *745*, 135621. https://doi.org/10.1016/j.neulet.2020.135621

Madisen, L., Zwingman, T. A., Sunkin, S. M., Oh, S. W., Zariwala, H. A., Gu, H., Ng, L. L., Palmiter, R. D., Hawrylycz, M. J., Jones, A. R., Lein, E. S., & Zeng, H. (2010). A robust and high-throughput Cre reporting and characterization system for the whole mouse brain. *Nature Neuroscience*, *13*(1), 133–140. https://doi.org/10.1038/nn.2467

Manvich, D. F., Webster, K. A., Foster, S. L., Farrell, M. S., Ritchie, J. C., Porter, J. H., & Weinshenker, D. (2018). The DREADD agonist clozapine N-oxide (CNO) is reverse-metabolized to clozapine and produces clozapine-like interoceptive stimulus effects in rats and mice. *Scientific Reports*, *8*(1), Article 1. https://doi.org/10.1038/s41598-018-22116-z

Maren, S., & Holt, W. (2000). The hippocampus and contextual memory retrieval in Pavlovian conditioning. *Behavioural Brain Research*, *110*(1–2), Article 1–2. https://doi.org/10.1016/S0166-4328(99)00188-6

Maren, S., Phan, K. L., & Liberzon, I. (2013). The contextual brain: Implications for fear conditioning, extinction and psychopathology. *Nature Reviews. Neuroscience*, *14*(6), 417–428. https://doi.org/10.1038/nrn3492

Maren, S., & Quirk, G. J. (2004). Neuronal signalling of fear memory. *Nature Reviews Neuroscience*, *5*(11), 844–852. https://doi.org/10.1038/nrn1535

McKenna, J. T., & Vertes, R. P. (2004). Afferent projections to nucleus reuniens of the thalamus. *The Journal of Comparative Neurology*, *480*(2), 115–142. https://doi.org/10.1002/cne.20342

Milekic, M. H., & Alberini, C. M. (2002). Temporally graded requirement for protein synthesis following memory reactivation. *Neuron*, *36*(3), 521–525. https://doi.org/10.1016/s0896-6273(02)00976-5

Moscovitch, M., Nadel, L., Winocur, G., Gilboa, A., & Rosenbaum, R. S. (2006). The cognitive neuroscience of remote episodic, semantic and spatial memory. *Current Opinion in Neurobiology*, *16*(2), 179–190. https://doi.org/10.1016/j.conb.2006.03.013

Müller, C., & Remy, S. (2018). Septo-hippocampal interaction. *Cell and tissue research, 373*(3), 565–575. https://doi.org/10.1007/s00441-017-2745-2

Myers, K. M., & Davis, M. (2002). Behavioral and Neural Analysis of Extinction. *Neuron*, *36*(4), 567–584. https://doi.org/10.1016/S0896-6273(02)01064-4

Nyakas, C., Luiten, P. G., Spencer, D. G., & Traber, J. (1987). Detailed projection patterns of septal and diagonal band efferents to the hippocampus in the rat with emphasis on innervation of CA1 and dentate gyrus. *Brain Research Bulletin*, *18*(4), 533–545. https://doi.org/10.1016/0361-9230(87)90117-1

Orsini, C. A., & Maren, S. (2012). Neural and cellular mechanisms of fear and extinction memory formation. *Neuroscience and Biobehavioral Reviews*, *36*(7), 1773–1802. https://doi.org/10.1016/j.neubiorev.2011.12.014

Paxinos, George, and Keith B. J Franklin. Paxinos and Franklin's the Mouse Brain in Stereotaxic Coordinates. 5th ed., Elsevier Academic Press, 2019.

Phillips, R. G., & LeDoux, J. E. (1992). Differential contribution of amygdala and hippocampus to cued and contextual fear conditioning. *Behavioral neuroscience*, *106*(2), 274–285. https://doi.org/10.1037//0735-7044.106.2.274

Preston, A. R., & Eichenbaum, H. (2013). Interplay of hippocampus and prefrontal cortex in memory. *Current Biology: CB*, *23*(17), R764-773. https://doi.org/10.1016/j.cub.2013.05.041

Quet, E., Majchrzak, M., Cosquer, B., Morvan, T., Wolff, M., Cassel, J.-C., Pereira de Vasconcelos, A., & Stéphan, A. (2020). The reuniens and rhomboid nuclei are necessary for contextual fear memory persistence in rats. *Brain Structure & Function*, *225*(3), 955–968. https://doi.org/10.1007/s00429-020-02048-z

Radwanska, K., Medvedev, N. I., Pereira, G. S., Engmann, O., Thiede, N., Moraes, M. F. D., Villers, A., Irvine, E. E., Maunganidze, N. S., Pyza, E. M., Ris, L., Szymańska, M., Lipiński, M., Kaczmarek, L., Stewart, M. G., & Giese, K. P. (2011). Mechanism for long-term memory formation when synaptic strengthening is impaired. *Proceedings of the National Academy of Sciences of the United States of America*, *108*(45), 18471–18475. https://doi.org/10.1073/pnas.1109680108

Radwanska, K., Schenatto-Pereira, G., Ziółkowska, M., Łukasiewicz, K., & Giese, K. P. (2015). Mapping fear memory consolidation and extinction-specific expression of JunB. *Neurobiology of Learning and Memory*, *125*, 106–112. https://doi.org/10.1016/j.nlm.2015.08.007

Ramanathan, K. R., Jin, J., Giustino, T. F., Payne, M. R., & Maren, S. (2018). Prefrontal projections to the thalamic nucleus reuniens mediate fear extinction. *Nature Communications*, *9*(1), 4527. https://doi.org/10.1038/s41467-018-06970-z

Ramanathan, K. R., & Maren, S. (2019). Nucleus reuniens mediates the extinction of contextual fear conditioning. *Behavioural Brain Research*, *374*, 112114. https://doi.org/10.1016/j.bbr.2019.112114

Ratigan, H. C., Krishnan, S., Smith, S., & Sheffield, M. E. J. (2023). A thalamic-hippocampal CA1 signal for contextual fear memory suppression, extinction, and discrimination. *Nature Communications*, *14*(1), 6758. https://doi.org/10.1038/s41467-023-42429-6

Roy, A., Svensson, F. P., Mazeh, A., & Kocsis, B. (2017). Prefrontal-hippocampal coupling by theta rhythm and by 2–5 Hz oscillation in the delta band: The role of the nucleus reuniens of the thalamus. *Brain Structure & Function*, *222*(6), 2819–2830. https://doi.org/10.1007/s00429-017-1374-6

Scheel, N., Wulff, P., & de Mooij-van Malsen, J. G. (2020). Afferent connections of the thalamic nucleus reuniens in the mouse. *The Journal of Comparative Neurology*, *528*(7), 1189–1202. https://doi.org/10.1002/cne.24811

Silva, B. A., Astori, S., Burns, A. M., Heiser, H., van den Heuvel, L., Santoni, G., Martinez-Reza, M. F., Sandi, C., & Gräff, J. (2021). A thalamo-amygdalar circuit underlying the extinction of remote fear memories. *Nature Neuroscience*, *24*(7), 964–974. https://doi.org/10.1038/s41593-021-00856-y

Simons, J. S., & Spiers, H. J. (2003). Prefrontal and medial temporal lobe interactions in long-term memory. *Nature Reviews. Neuroscience*, *4*(8), 637–648. https://doi.org/10.1038/nrn1178

Smith, K. S., Bucci, D. J., Luikart, B. W., & Mahler, S. V. (2016). DREADDs: Use and Application in Behavioral Neuroscience. *Behavioral Neuroscience*, *130*(2), 137–155. https://doi.org/10.1037/bne0000135

Squire, L. R., & Alvarez, P. (1995). Retrograde amnesia and memory consolidation: A neurobiological perspective. *Current Opinion in Neurobiology*, *5*(2), 169–177. https://doi.org/10.1016/0959-4388(95)80023-9

Tanaka, K. Z., Pevzner, A., Hamidi, A. B., Nakazawa, Y., Graham, J., & Wiltgen, B. J. (2014). Cortical Representations Are Reinstated by the Hippocampus during Memory Retrieval. *Neuron*, *84*(2), 347–354. https://doi.org/10.1016/j.neuron.2014.09.037

Tao, S., Wang, Y., Peng, J., Zhao, Y., He, X., Yu, X., Liu, Q., Jin, S., & Xu, F. (2021). Whole-Brain Mapping the Direct Inputs of Dorsal and Ventral CA1 Projection Neurons. *Frontiers in Neural Circuits*, *15*, 643230. https://doi.org/10.3389/fncir.2021.643230

Tonegawa, S., Morrissey, M. D., & Kitamura, T. (2018). The role of engram cells in the systems consolidation of memory. *Nature Reviews. Neuroscience*, *19*(8), 485–498. https://doi.org/10.1038/s41583-018-0031-2

Totty, M. S., Tuna, T., Ramanathan, K. R., Jin, J., Peters, S. E., & Maren, S. (2023). Thalamic nucleus reuniens coordinates prefrontal-hippocampal synchrony to suppress extinguished fear. *Nature Communications*, *14*(1), 6565. https://doi.org/10.1038/s41467-023-42315-1

Tronson, N. C., Schrick, C., Guzman, Y. F., Huh, K. H., Srivastava, D. P., Penzes, P., Guedea, A. L., Gao, C., & Radulovic, J. (2009). Segregated Populations of Hippocampal Principal CA1 Neurons Mediating Conditioning and Extinction of Contextual Fear. *Journal of Neuroscience*, *29*(11), 3387–3394. https://doi.org/10.1523/JNEUROSCI.5619-08.2009

Troyner, F., & Bertoglio, L. J. (2021). Nucleus reuniens of the thalamus controls fear memory reconsolidation. *Neurobiology of Learning and Memory*, *177*, 107343. https://doi.org/10.1016/j.nlm.2020.107343

Unal, G., Joshi, A., Viney, T. J., Kis, V., & Somogyi, P. (2015). Synaptic Targets of Medial Septal Projections in the Hippocampus and Extrahippocampal Cortices of the Mouse. *The Journal of neuroscience: the official journal of the Society for Neuroscience*, *35*(48), 15812–15826. https://doi.org/10.1523/JNEUROSCI.2639-15.2015

Vasudevan, K., Ramanathan, K. R., Vierkant, V., & Maren, S. (2022). Nucleus reuniens inactivation does not impair consolidation or reconsolidation of fear extinction. *Learning & Memory*, *29*(8), 216–222. https://doi.org/10.1101/lm.053611.122

Venkataraman, A., Hunter, S. C., Dhinojwala, M., Ghebrezadik, D., Guo, J., Inoue, K., Young, L. J., & Dias, B. G. (2021). Incerto-thalamic modulation of fear via GABA and dopamine. *Neuropsychopharmacology: Official Publication of the American College of Neuropsychopharmacology*, *46*(9), 1658–1668. https://doi.org/10.1038/s41386-021-01006-5

Vertes, R. P., Hoover, W. B., Do Valle, A. C., Sherman, A., & Rodriguez, J. J. (2006). Efferent projections of reuniens and rhomboid nuclei of the thalamus in the rat. *The Journal of Comparative Neurology*, *499*(5), 768–796. https://doi.org/10.1002/cne.21135

Vetere, G., Kenney, J. W., Tran, L. M., Xia, F., Steadman, P. E., Parkinson, J., Josselyn, S. A., & Frankland, P. W. (2017). Chemogenetic Interrogation of a Brain-wide Fear Memory Network in Mice. *Neuron*, *94*(2), 363–374.e4. https://doi.org/10.1016/j.neuron.2017.03.037

Vetere, G., Xia, F., Ramsaran, A. I., Tran, L. M., Josselyn, S. A., & Frankland, P. W. (2021). An inhibitory hippocampal–thalamic pathway modulates remote memory retrieval. *Nature Neuroscience*, *24*(5), 685–693. https://doi.org/10.1038/s41593-021-00819-3

Wheeler, A. L., Teixeira, C. M., Wang, A. H., Xiong, X., Kovacevic, N., Lerch, J. P., McIntosh, A. R., Parkinson, J., & Frankland, P. W. (2013). Identification of a Functional Connectome for Long-Term Fear Memory in Mice. *PLOS Computational Biology*, *9*(1), e1002853. https://doi.org/10.1371/journal.pcbi.1002853

Xiao, C., Liu, Y., Xu, J., Gan, X., & Xiao, Z. (2018). Septal and Hippocampal Neurons Contribute to Auditory Relay and Fear Conditioning. *Frontiers in cellular neuroscience*, *12*, 102. https://doi.org/10.3389/fncel.2018.00102

Xu, W., & Sudhof, T. C. (2013). A Neural Circuit for Memory Specificity and Generalization. *Science*, *339*(6125), 1290–1295. https://doi.org/10.1126/science.1229534

Yanakieva, S., Mathiasen, M. L., Amin, E., Nelson, A. J. D., O'Mara, S. M., & Aggleton, J. P. (2022). Collateral rostral thalamic projections to prelimbic, infralimbic, anterior cingulate and retrosplenial cortices in the rat brain. *The European Journal of Neuroscience*, *56*(10), 5869–5887. https://doi.org/10.1111/ejn.15819

Zingg, B., Chou, X.-L., Zhang, Z.-G., Mesik, L., Liang, F., Tao, H. W., & Zhang, L. I. (2017). AAV-Mediated Anterograde Transsynaptic Tagging: Mapping Corticocollicular Input-Defined Neural Pathways for Defense Behaviors. *Neuron*, *93*(1), 33–47. https://doi.org/10.1016/j.neuron.2016.11.045

Ziółkowska, M., Sotoudeh, N., Cały, A., Puchalska, M., Pagano, R., Śliwińska, M. A., Salamian, A., & Radwanska, K. (2025). Projections from thalamic nucleus reuniens to hippocampal CA1 area participate in context fear extinction by affecting extinction-induced molecular remodeling of excitatory synapses. *eLife*, *13*, RP101736. https://doi.org/10.7554/eLife.101736

# SUPPLEMENTARY MATERIALS

Supplementary Fig. 1. Experimental design for c-Fos analysis. (A) Experimental groups. Naive mice were taken from their home cage. 5US group underwent CFC with 5 electric shocks in novel context and were sacrificed 1 day later. Ctx mice were exposed twice to the novel context without US experience and were sacrificed 70 minutes after the last exposure. Recent groups underwent CFC and a contextual fear extinction session 1 day after CFC, and were sacrificed 70 minutes after the extinction. Remote groups underwent CFC and a contextual fear extinction session 30 days after CFC, and were sacrificed 70 minutes after the extinction. Mice brains were sliced and used for c-Fos immunostaining. (B) Analised brain regions. PrL, prelimbic cortex; IL, infralimbic cortex; CG, cingulate cortex; RSG, retrosplenial cortex, granular part; RSA, retrosplenial cortex, agranular part; V1, primary visual cortex; ENT, entorhinal cortex; LS, lateral septum; MS, medial septum; AD, anterodorsal nucleus of thalamus; AV, anteroventral nucleus of thalamus; AM, anteromedial nucleus of thalamus; LD, laterodorsal nucleus of thalamus; RE, nucleus reuniens; CM, centromedial nucleus of thalamus; MD, mediodorsal nucleus of thalamus; PV, paraventricular nucleus of thalamus; CA1, dorsal hippocampus, CA1 area; CA3, dorsal hippocampus, CA3 area; DG, dentate gyrus; BLA, basolateral nucleus of the amygdala; LA, lateral nucleus of the amygdala; CeA, central nucleus of the amygdala, capsular and lateral divisions; CeM, central nucleus of the amygdala, centromedial division. (C) Representative microphotographs of c-Fos immunostaining in the analyzed brain regions.

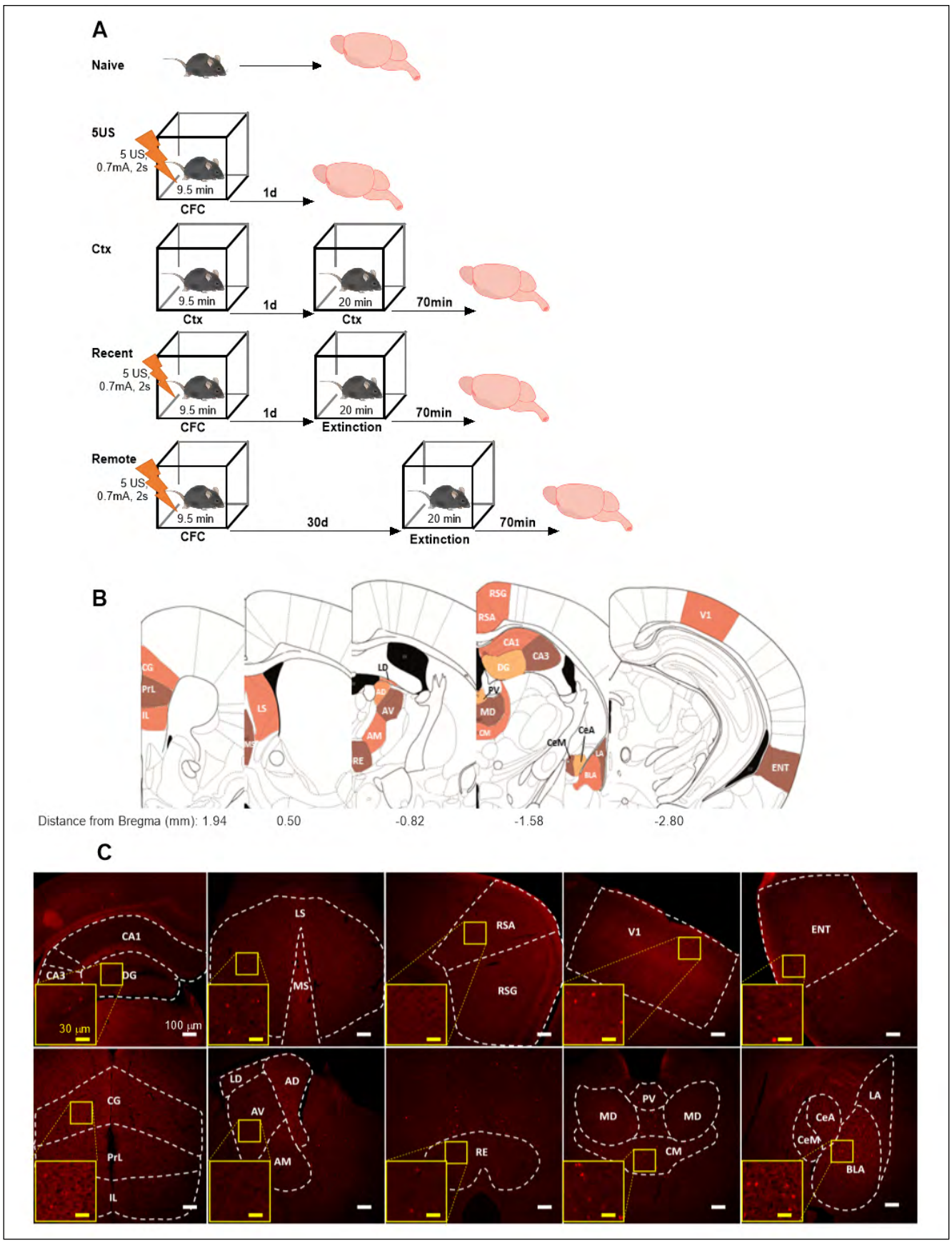
A
Naive
5US
5 US,
0.7mA, 2s
9.5 min
CFC
1d
Ctx
9.5 min
Ctx
1d
20 min
Ctx
70min
Recent
5 US,
0.7mA, 2s
9.5 min
CFC
1d
20 min
Extinction
70min
Remote
5 US,
0.7mA, 2s
9.5 min
CFC
30d
20 min
Extinction
70min
B
RSG
RSA
V1
CG
PrL
IL
LD
AD
AV
AM
RE
LS
MS
CA1
CA3
DG
PV
MD
CM
CeM
CeA
LA
BLA
ENT
Distance from Bregma (mm): 1.94
0.50
-0.82
-1.58
-2.80
C
CA1
CA3
DG
30 μm
100 μm
LS
MS
RSA
RSG
V1
ENT
CG
PrL
IL
LD
AD
AV
AM
RE
MD
PV
MD
CM
LA
CeA
CeM
BLA

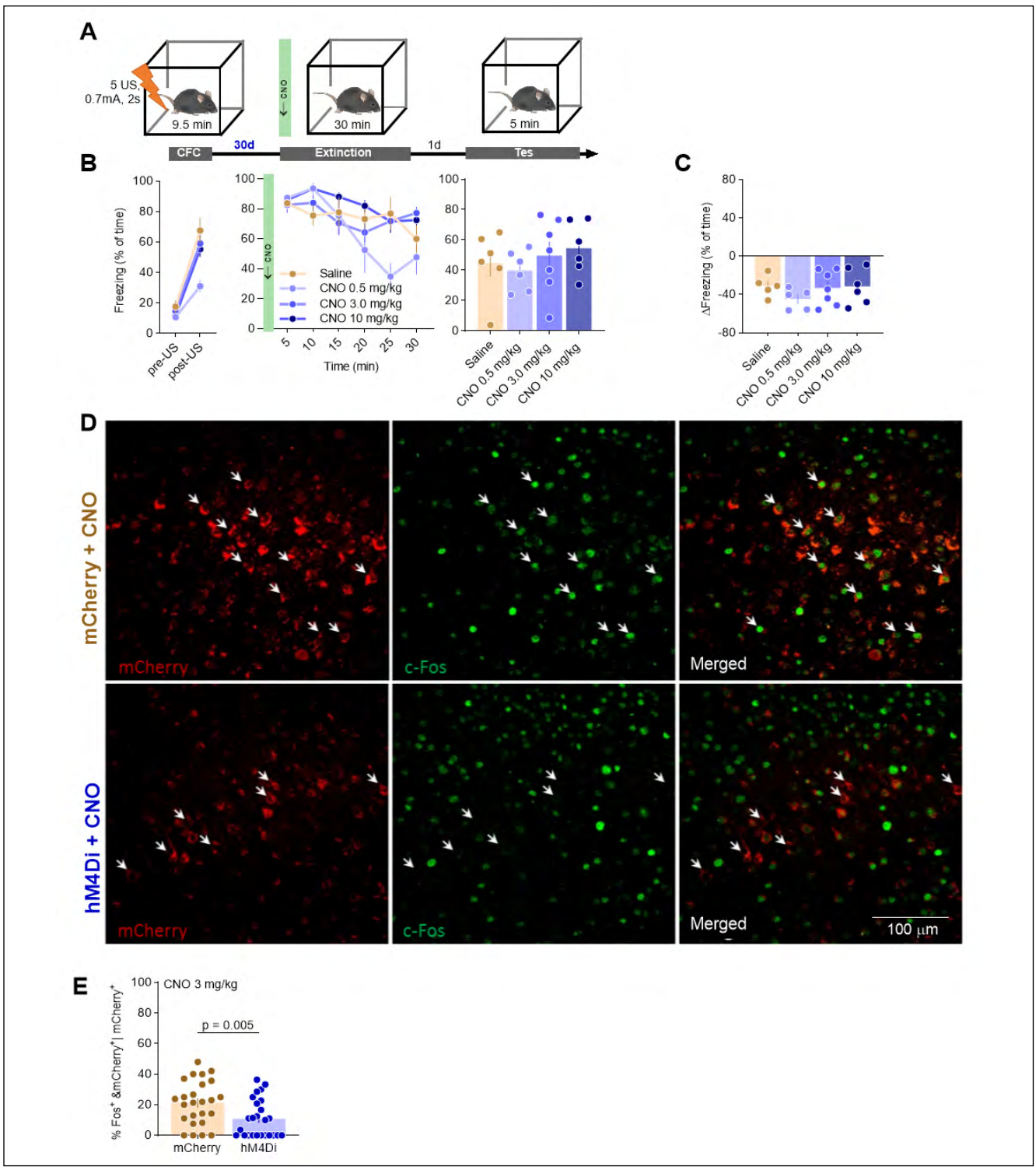


Supplementary Fig. 2. Validation of chemogenetic tools. (A) Experimental timeline. C57BL/6J mice (without hM4Di expression) underwent CFC and 30 days later they were injected with CNO (0.5, 3 or 10 mg/kg) or saline. Thirty minutes later they were exposed to the training context for contextual fear memory extinction and fear extinction memory was tested in the same context one day later. (B) Summary of data for freezing levels during CFC (CFC: RM ANOVA, effect of time: $F_{(1, 21)}$=270, P<0.001), remote fear memory extinction session (Extinction: RM ANOVA, effect of time: $F_{(3.66, 69.5)}$=11.2, P<0.001; effect of treatment: $F_{(3, 19)}$=2.59, P=0.083) and fear extinction test (Test: one-way ANOVA, $F_{(3, 21)}$=0.613, P=0.614). (C) Summary of data showing the change of freezing frequency during Test (T) as compared to the first 5 minutes of the Extinction (E5) (unpaired t-test: one-way ANOVA, $F_{(3, 19)}$=0.846, P=0.486). (D-E) Analysis of the efficiency of chemogenetic inhibition. (D) Representative microphotographs of c-Fos immunostaining and hM4Di and mCherry expression in V1. (E) Summary of data analysis for the frequency of c-Fos$^+$ cells among the cells transduced with hM4Di or mCherry (Mann-Whitney U=183, P=0.005).

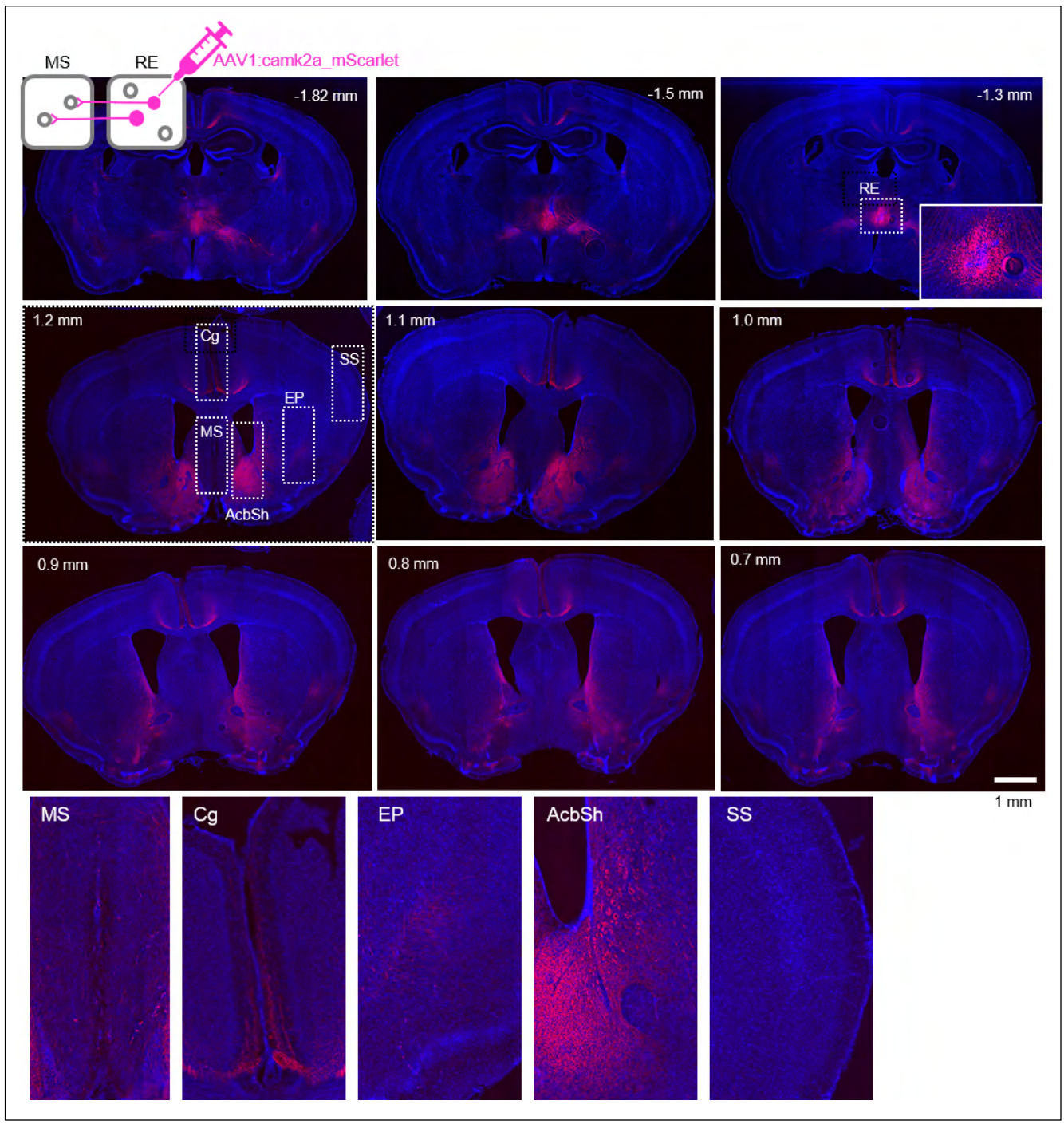


Supplementary Fig. 3. Identification of anatomical projections from RE to MS. C57BL/6j mice were injected into RE with AAV1: camk2a_mScarlet resulting in mScarlet expression in RE neurons and their projections. Strong mScarlet signal was observed in AcbSh, weak signal was found in MS, Cg, and AI, no signal was found in SS. AcbSh, nucleus accumbens shell; Cg, cingulate cortex; EP, endopiriform nucleus; MS, medial septum; SS, somatosensory cortex. Brain coordinates according to Bregma are indicated.